GEOLOGICAL JOURNAL
Geol. J. **48**: 170–193 (2013)
Published online 29 May 2012 in Wiley Online Library
(wileyonlinelibrary.com). DOI: 10.1002/gj.2425

New conodont species and biostratigraphy of the Santa Rosita Formation (upper Furongian–Tremadocian) in the Tilcara Range, Cordillera Oriental of Jujuy, Argentina

FERNANDO J. ZEBALLO* and GUILLERMO L. ALBANESI

CICTERRA-CONICET—Museo de Paleontología, Facultad de Ciencias Exactas, Físicas y Naturales, Universidad Nacional de Córdoba, Av. Vélez Sarsfield 299, (5000) Córdoba, Argentina

A new conodont collection from the Alfarcito area of the Tilcara Range, Cordillera Oriental of northwestern Argentina, has been studied. The Santa Rosita Formation exposed in this area consists of the Tilcara, Casa Colorada, Pico de Halcón, Alfarcito, Rupasca and Humacha members, which have a combined total thickness of *ca*. 1100 m. The sequence is composed of interbedded shales and sandstones, including calcarenites and coquinas, mostly appearing in the upper parts of the units. An abundant fauna of conodonts (*ca*. 11 000 elements), associated with graptolites and trilobites, was recorded. The biostratigraphic analysis allows for the identification of the *Cordylodus intermedius* and *C. lindstromi sensu lato* zones at the base of the Alfarcito Member. The *C. angulatus* Zone spans the upper part of the latter unit, and the *Paltodus deltifer* Zone (*Paltodus deltifer pristinus* and *P. deltifer deltifer* subzones) is identified in the Rupasca and Humacha members. The new species *Acanthodus raqueli*, *A. humachensis*, *Utahconus tortibasis*, *U. scandodiformis*, *U. purmamarcensis*, *Variabiloconus crassus*, *Kallidontus gondwanicus* and *Acodus primitivus* are recorded from the two latter biozones and they are described herein. The genera *Acanthodus* and *Variabiloconus* are emended, and a new genus *Tilcarodus* is created to include *T. humahuacensis* (Albanesi and Aceñolaza). Copyright © 2012 John Wiley & Sons, Ltd.

Received 11 August 2011; accepted 29 February 2012

KEY WORDS conodonts; biostratigraphy; Cambrian; Ordovician; Cordillera Oriental, Argentina

1. INTRODUCTION

The Santa Rosita Formation, late Cambrian–Early Ordovician in age, which is exposed along the eastern margin of the Quebrada de Humahuaca, was systematically sampled for fossils, particularly searching for conodonts, graptolites and trilobites. The study area is located in the eastern margin of the Cordillera Oriental, northwestern Argentina; it is bounded by the Sierras Subandinas to the east and by the Grande River to the west (Figure 1A, B). The Cambro-Ordovician outcrops of the Santa Rosita Formation that were surveyed in this work have a NNE–SSW strike, involving the Tilcara Range and the Alfarcito Hills, which extend between the parallels S 23° 21′ 25″ and S 23° 52′ 00″ (Figure 1B).

The first geological studies of the Cordillera Oriental were accomplished by Brackebusch (1883, 1892), Keidel (1910, 1943), Hausen (1925), Schlagintweit (1937) and Groeber (1938). After these pioneering studies, numerous authors have produced works at regional scale for this geological province (e.g. Turner and Mon, 1979; Ramos, 1999; Moya, 2008; Astini, 2003, 2008). The first papers devoted to the study area were those of Bonarelli (1921) and Feruglio (1931), who described geological profiles across the Tilcara Range. The important publication by Harrington and Leanza (1957) regarding trilobites, considered the Casa Colorada, Rupasca and San Gregorio sections, where they referred to the Ordovician rocks cropping out in the Alfarcito area as the 'Casa Colorada Shales', 'Alfarcito Limestones' and 'Rupasca Shales'. These authors also described the 'Purmamarca Shales', 'Chañarcito Limestones' and 'Coquena Limestones' in the nearby town of Purmamarca. López and Nullo (1969) carried out a geological and palaeontological survey in the area between the Maimará and Huacalera localities, providing a detailed description for the stratigraphic units previously mentioned by Harrington and Leanza (1957). In her doctoral dissertation, Moya (1988a) analyzed the geology of some sections from the eastern flank of the Humahuaca Creek; e.g. Angosto de Chucalezna, Rupasca and Conglomerado creeks, as well as Ordovician sequences exposed in the Abra Blanca area, Tres Ciénagas, Campo

*Correspondence to: F. J. Zeballo, Museo de Paleontología, Facultad de Ciencias Exactas, Físicas y Naturales, Universidad Nacional de Córdoba, Casilla de Correo 1598, 5000 Córdoba, Argentina. E-mail: fzeballo@hotmail.com

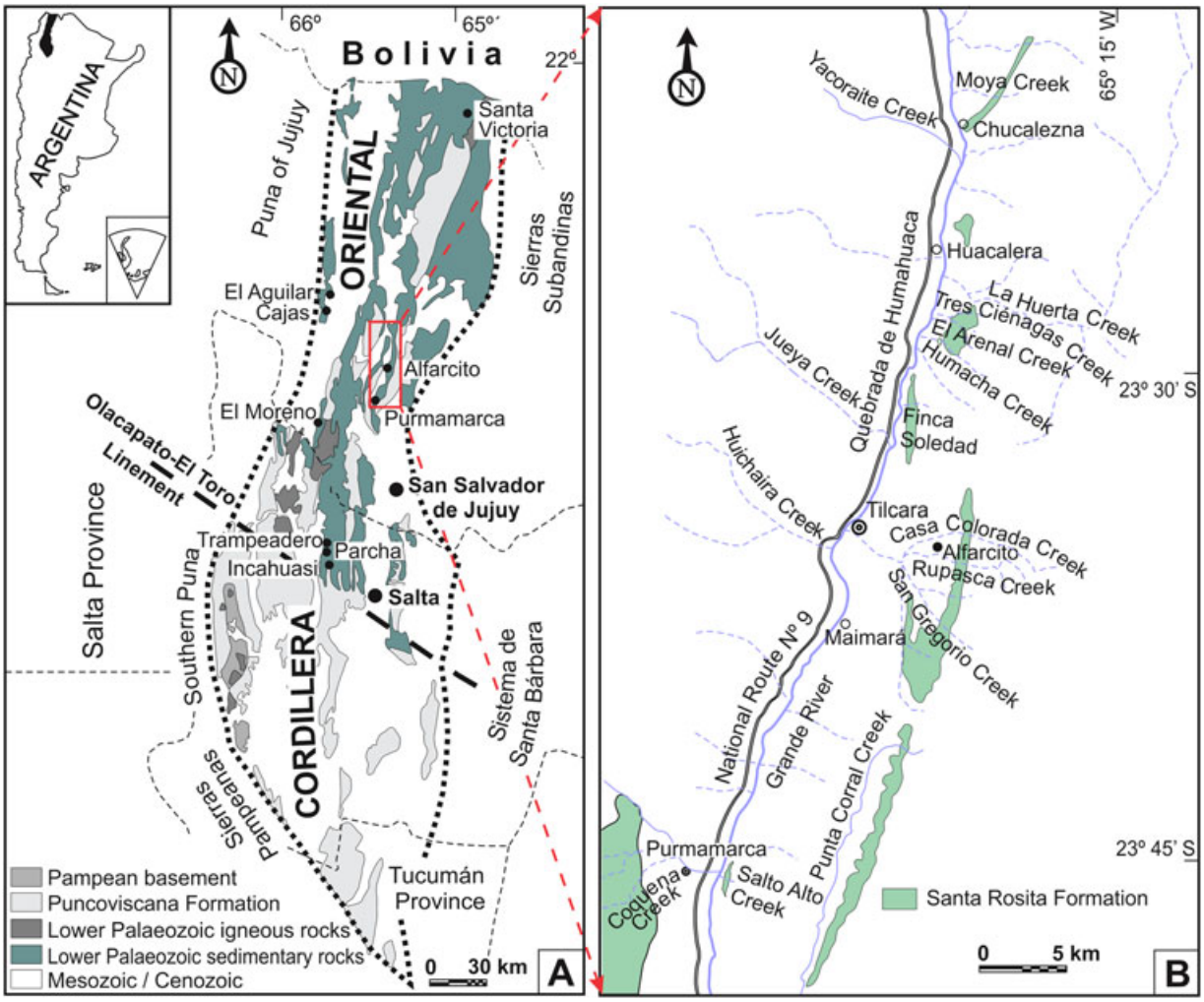

Figure 1. (A) Study area in the Argentine Cordillera Oriental and (B) Cambro-Ordovician outcrops of the Santa Rosita Formation (modified from Zeballo *et al*., 2011). This figure is available in colour online at wileyonlinelibrary.com/journal/gj

Grande, El Arenal and Humacha creeks, which was partly published later (Moya, 1988b).

Related works about conodonts in different areas of the Cordillera Oriental were carried out by Rao and Hünicken (1995), Rao and Flores (1998), Rao (1999), Tortello *et al*. (1999) and Rao *et al*. (1994), among others. The correlation between the conodont and graptolite associations of the Alfarcito area was first proposed by Zeballo *et al*. (2005a, b). In turn, Zeballo and Tortello (2005) analyzed the trilobite association for the same region. Albanesi and Aceñolaza (2005) studied the conodont fauna and associated trace fossils of the Rupasca Member in the western flank of the Angosto de Chucalezna, having verified a similar faunal association to that published by Zeballo *et al*. (2005b). An integrated study of the fossil fauna using the sequence stratigraphy framework was carried out by Buatois *et al*. (2006), who formally proposed a division of the Santa Rosita Formation into six members.

The present contribution is aimed at updating the Ordovician conodont biostratigraphy of the Cordillera Oriental, which is linked to key graptolite and trilobite data, allowing high-resolution correlations to be made at regional and global levels. Furthermore, 8 new conodont species and a new conodont genus are defined. The diagnoses of the genera *Acanthodus* and *Variabiloconus* are emended in the light of the new recorded material.

2. MATERIALS AND METHODS

An extensive search for graptolites and trilobites was carried out in the shaly Ordovician sequences of the study area. At the same time, carbonate samples (calcarenites and coquinas) for conodonts, 2–3 kg each, were taken with precise stratigraphic locations. Graptolites and trilobites were recorded from 82 samples, and the 116 calcareous rock samples that in total weighed about 260 kg, yielded *ca*. 11 000

conodont elements (5163 of those elements correspond to the species described herein; Appendix, tables 1, 2) showing conodont alteration index values (CAI) 2–3.

In this work the Moya, Chucalezna, Tres Ciénagas, El Arenal, Humacha, Casa Colorada, San Gregorio, Punta Corral, Salto Alto, Coquena, Chalala and Trampeadero sections are analyzed (abbreviated as Moya, Chuc, TrCi, ElAr, Hum, CC, SG, PtaCorral, Purm, Coq, Chal, and Tramp, respectively). Conodonts of the genus *Kallidontus* from the Tiñú Formation (Mexico) are compared with Argentinian collections and some of them are illustrated herein.

The conodont recovery followed acetic acid etching by conventional techniques of the carbonate samples (Stone, 1987). Shaly samples were processed by thermic–mechanic methodologies (Jeppsson *et al*., 1999); however, these types of rocks did not yield conodonts. The insoluble residue was concentrated by means of organic heavy liquids and the heavy fraction was examined for microfossils (Pokorny, 1963).

The sampled rocks were processed in the Micropalaeontology Laboratory, FCEFyN, of the National University of Córdoba, and the studied fossil material is housed in the Museum of Palaeontology under the repository code CORD-MP for microfossils and CORD-PZ for macrofossils.

3. GEOLOGIC AND STRATIGRAPHIC FRAMEWORK

The Central Andean Basin covers parts of the Jujuy, Salta, Tucumán and Catamarca provinces in Argentina. It comprises the geological provinces of the Puna, Cordillera Oriental, and Sierras Subandinas, as well as the Sistema de Santa Bárbara (Ramos, 1999). Traditionally, these units have been considered as separate basins. However, following Astini (2003), there is no stratigraphic evidence to support this approach. According to his criteria they are grouped as the northwest basins that would also cover the basement of the Chaco plains. This basin represents the southern end of the Central Andean Basin that stretches into neighbouring countries in the Cordillera Oriental and Cordillera Central of Bolivia and Peru.

The Ordovician deposits are better represented in the Cordillera Oriental (Brackebusch, 1892), and they exhibit a gradual increase in thickness towards the north (Astini, 2003). They are exposed in the Santa Victoria, Zenta, Cochinoca, Aguilar, Tilcara, and Mojotoro ranges. This geological province consists of rugged mountain ranges separated by deep valleys (valleys at 500 m altitude and the highest peaks over 6000 m) (Turner and Mon, 1979). It is characterized by large thrust belts of Lower Palaeozoic rocks juxtaposed on a Neoproterozoic–Early Palaeozoic basement of metamorphic rocks of the Puncoviscana Formation (Ramos, 1999). The latter unit is composed of dark-coloured fine-grained sediments (mudstones and subordinate psammitic rocks) of low-grade metamorphism (slates and meta-greywackes). It has an apparent thickness of *ca*. 5000 m near the Las Ovejas Mountain and is highly folded and deformed, making it impossible to know its actual thickness.

Above this formation lays the Mesón Group of Terreneuvian to middle Cambrian age, with a sharp angular unconformity. This discordance is seen notably in the Garganta del Diablo, at the headwaters of the Huasamayo River that borders the city of Tilcara (where the name is taken for the Tilcárica discordance, referring to the orogenic movements; i.e. the Tilcara phase). The Mesón Group consists of the Lizoite, Campanario and Chalhualmayoc formations, of predominantly sandstone composition. Amengual and Zanettini (1974) described a basal conglomerate for this group with 5–10 cm clasts of quartz, slate and quartzite from the underlying unit. This group with a thickness of about 2000 m, along with the Puncoviscana Formation, is the summit of the Tilcara Range and Alfarcito Hills.

The Santa Victoria Group (Furongian–Middle Ordovician) crops out in this area represented only by the Santa Rosita Formation and its constituent members: the Tilcara, Casa Colorada, Pico de Halcón, Alfarcito, Rupasca and Humacha members (Buatois *et al*., 2006; Figure 2). The relationship with the Mesón Group is unconformable (Irúyica discordance) and can be observed in some sections (e.g. the Abra Blanca Creek) underlying a basal conglomerate composed of quartz and rocks from the Puncoviscana Formation and the Mesón Group, or coarse-grained sandstones wherever this is absent. The Santa Rosita Formation is completely exposed in the La Huerta gorge (comprising the Tres Ciénagas, El Arenal, and Humacha creeks), where the continuity of the sequence can be seen (*ca*. 1100 m thick). Throughout the whole of the Santa Rosita Formation are intercalated calcarenite levels and coquinas, usually associated with hummocky cross-stratified sandstone and tempestites (storm events), from which most of the microfossils studied in this work come from.

A major hiatus spanning the rest of the Palaeozoic and most of the Mesozoic separates the Santa Victoria Group and the Salta Group (late Cretaceous–early Cenozoic). This group is approximately 700 m thick (López and Nullo, 1969), and units represented in the study area correspond to the Yacoraite Formation of the Balbuena Subgroup and the Santa Bárbara Subgroup. The lithologies include oolitic limestone, calcareous claystones and calcareous sandstones. The overlying rocks are Cenozoic with a Quaternary cover, poorly consolidated in some cases.

4. BIOSTRATIGRAPHIC CONSIDERATIONS

In this contribution, we follow the biostratigraphic schemes provided by Albanesi *et al*. (2008), Waisfeld and Vaccari

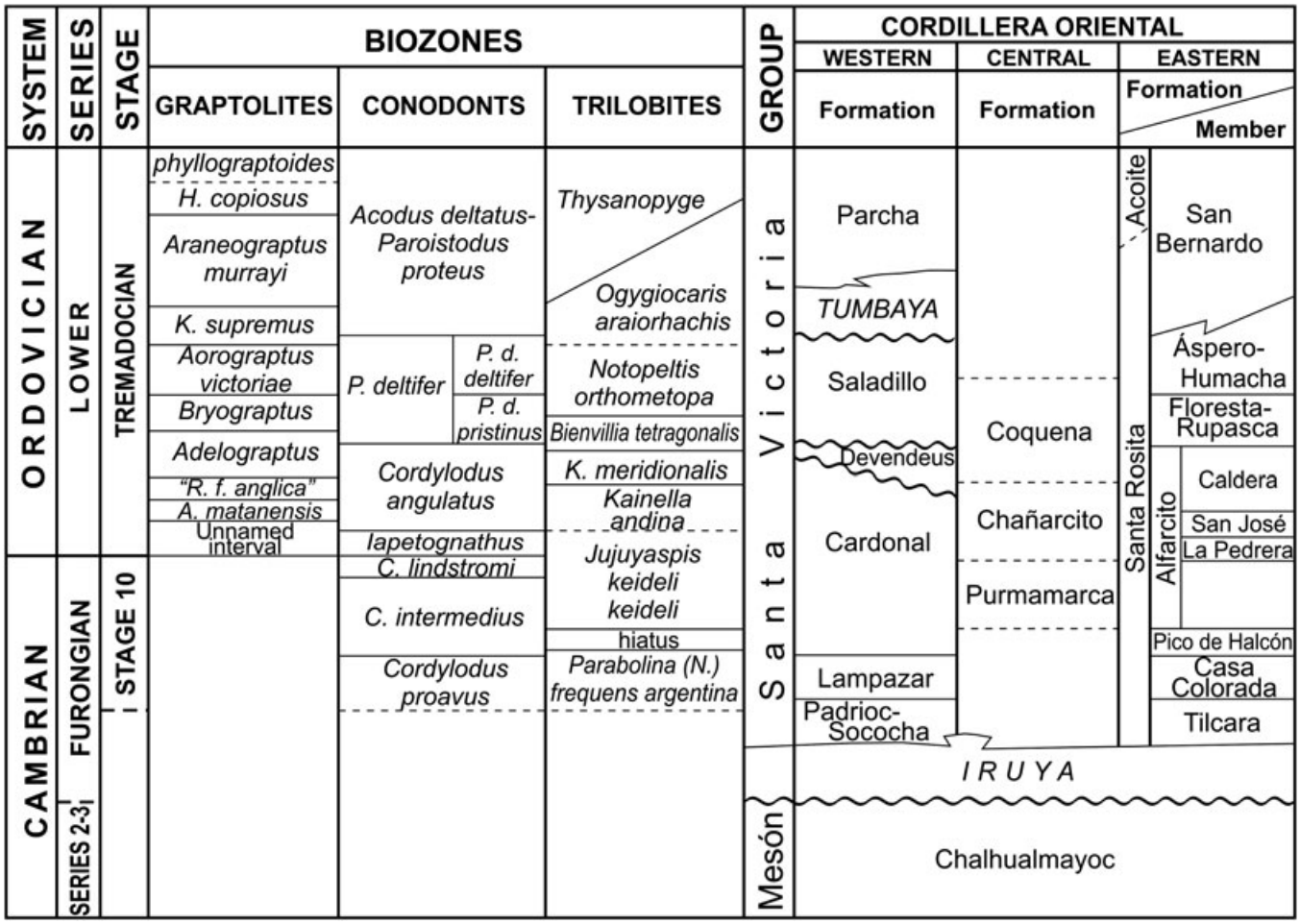

Figure 2. Conodont, graptolite and trilobite biostratigraphic scheme of the Furongian-Lower Ordovician related to lithostratigraphic units (modified after Harrington and Leanza, 1957; Albanesi *et al*., 2008; Waisfeld and Vaccari, 2008; Vaccari *et al*., 2010; Zeballo *et al*., 2011).

(2008), Zeballo and Albanesi (2009), and Zeballo *et al*. (2011). In these schemes, the *Cordylodus proavus* Zone (Figure 2) was identified in the Lampazar Formation at Cajas Range (Rao, 1999) and Angosto del Moreno (Albanesi in Moya *et al*., 2003), but it was still not recorded in the Tilcara Range, in the correlative Casa Colorada Member. On the other hand, the Tilcara and Pico de Halcón members are barren of conodonts, since these units were deposited in estuarine environments, under conditions unsuitable for conodont faunas.

The collection of conodonts recovered from the Santa Rosita Formation in the study area allows the identification of the *Cordylodus intermedius* Zone (*Hirsutodontus simplex* Subzone) at the base of the Alfarcito Member along with trilobites of the *Jujuyaspis keideli keideli* Zone (Zeballo and Albanesi, 2009). These data indicate that although the latter taxon has traditionally been viewed as a marker for the base of the Ordovician System (e.g. Aceñolaza, 1983; Aceñolaza and Aceñolaza, 1992), its lower range is actually Furongian in age (late Cambrian) (Figures 2 and 3).

The conodont *Cordylodus prolindstromi* Nicoll, 1991 (found in the Punta Corral Creek), suggests the presence of the *Cordylodus lindstromi sensu lato* Zone in the lower part of the Alfarcito Member, although the conodont association is poorly represented.

In contrast to the latter, the *Cordylodus angulatus* Zone is the best represented in terms of the number and variety of specimens, and most of the new species and their holotypes come from this biozone. It is recognized in the mid-upper section of the Alfarcito Member and base of the overlying Rupasca Member, associated with species of the graptolite genus *Adelograptus*, and various species of the trilobite genus *Kainella*. The *C. angulatus* Zone has also been identified in the Devendeus Formation, in the Trampeadero Creek (outside the study area), as well as in different sections of the Cordillera Oriental of Argentina (Zeballo *et al*., 2011).

The *Paltodus deltifer* Zone ranges through the upper part of the Santa Rosita Formation, with its two subzones (i.e. *Paltodus deltifer pristinus* and *P. deltifer deltifer*)

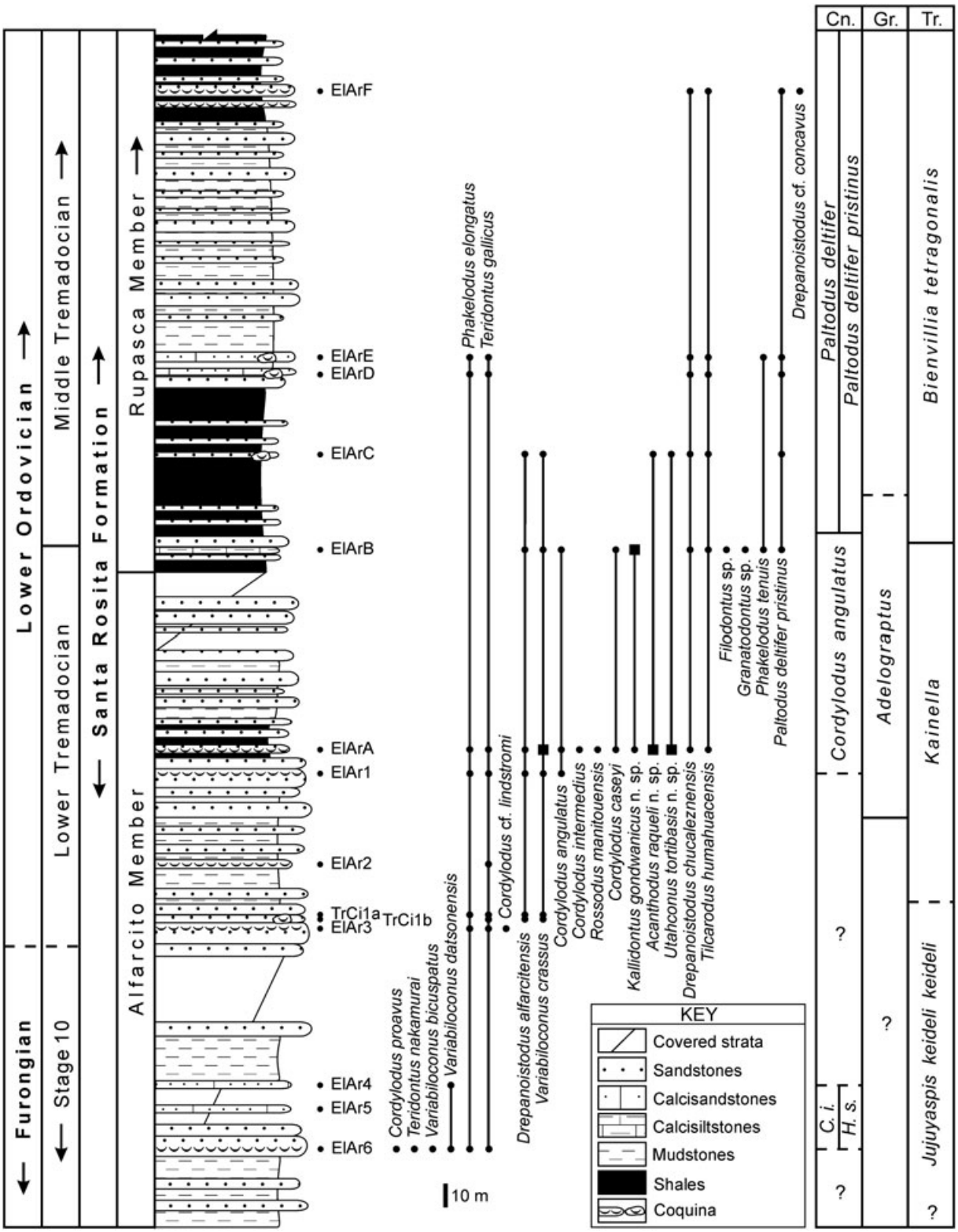

Figure 3. Stratigraphic column of the Alfarcito and Rupasca members (Santa Rosita Formation) from El Arenal section, with ranges of new species and the corresponding biozonation (Cn.: conodont zones and subzones; Gr.: graptolite zones; Tr.: trilobite zones; C. *i.: Cordylodus intermedius; H. s.: Hirsutodontus simplex;* solid squares: stratotype horizons of new species). The *C. i.–H. s.* biostratigraphic interval is correlated with that of the Salto Alto section published by Zeballo and Albanesi (2009).

distributed in the Rupasca Member and Humacha Member, respectively (Figures 2, 3, 4). Also, this biozone has been identified in the Coquena Formation, around the Purmamarca area (Zeballo *et al*., 2008) (Figure 5).

The chronostratigraphic scheme used in this contribution is that of Bergström *et al*. (2009), where the Ordovician System is divided in three series (Lower, Middle and Upper Ordovician) and seven stages. The Tremadocian Stage is divided in three Stage slices: Tr1, Tr2, and Tr3, marked by the first appearances of *Iapetognathus fluctivagus* Nicoll *et al*., 1999, *Paltodus deltifer pristinus* (Viira, 1970), and *Paroistodus proteus* (Lindström, 1955), respectively.

5. SYSTEMATIC PALAEONTOLOGY

Phylum CHORDATA Bateson, 1885
Superclass CONODONTA Pander, 1856
Class CONODONTI Branson, 1938
Subclass CAVIDONTI Sweet, 1988
Order PROCONODONTIDA Sweet, 1988
Family FRYXELLODONTIDAE Miller, 1980
Genus *Kallidontus* Pyle and Barnes, 2002

Type species. Kallidontus serratus Pyle and Barnes, 2002, original designation.

Kallidontus gondwanicus n. sp.
Figures 7V–Z, 9AC–AH

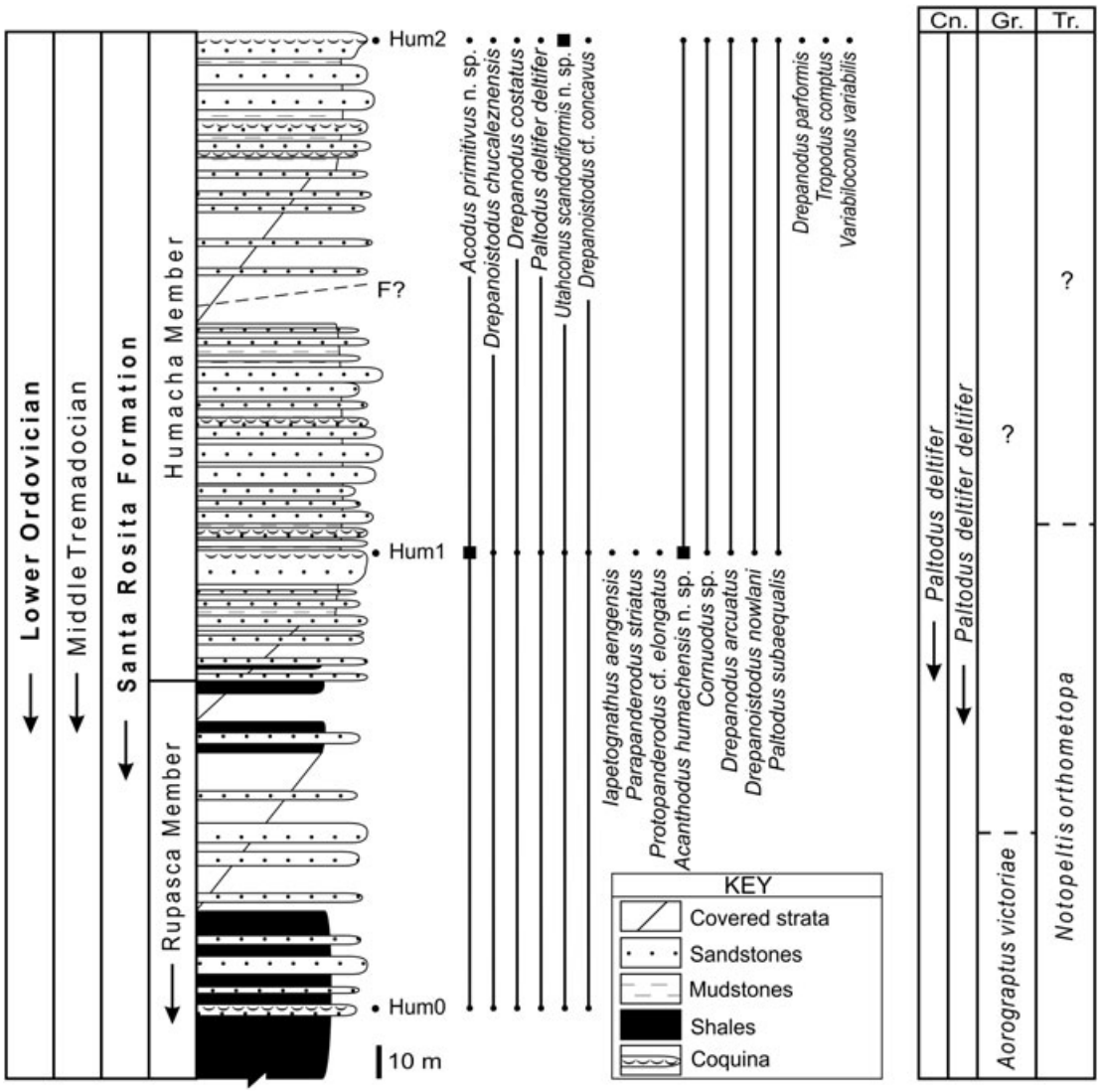

Figure 4. Stratigraphic column of the Rupasca and Humacha members (Santa Rosita Formation) from the Humacha section, with ranges of new species and the corresponding biozonation (Cn.: conodont zones and subzones; Gr.: graptolite zones; Tr.: trilobite zones; *P. d. p.: Paltodus deltifer pristinus;* solid square: stratotype horizons of new species).

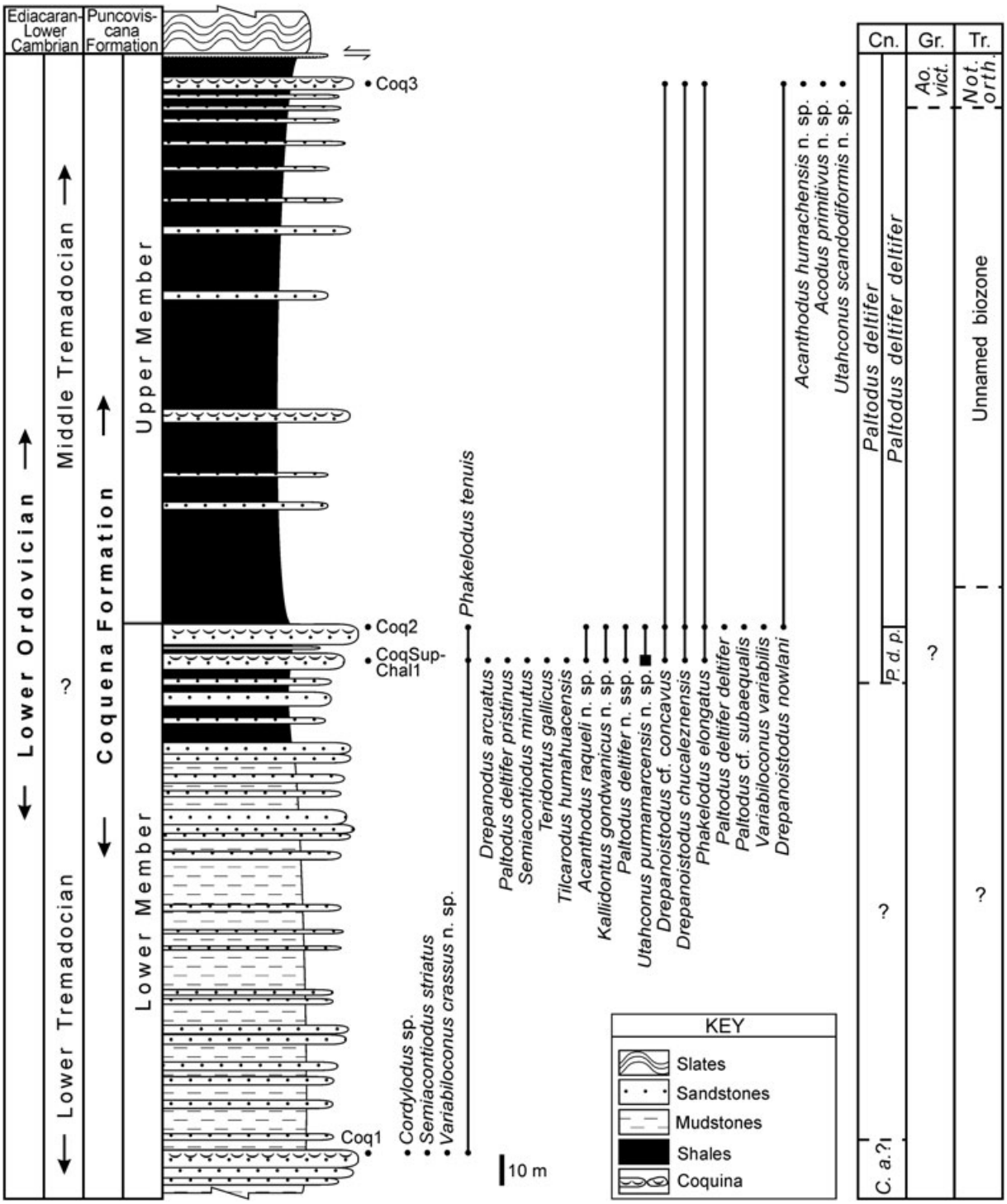

Figure 5. Stratigraphic column of the Coquena Formation from the Coquena and Chalala sections, with ranges of new species and the corresponding biozonation (Cn.: conodont zones and subzones; Gr.: graptolite zones; Tr.: trilobite zones; *C. a.: Cordylodus angulatus; P. d. p.: Paltodus deltifer pristinus; Ao. vict.: Aorograptus victoriae; Not. orth.: Notopeltis orthometopa;* solid square: stratotype horizons of new species).

?1999. *Distacodus* sp. Rao: 29; pl. 2, figs. 2, 5, 6.
2005b. *Coelocerodontus* sp. Zeballo *et al*.: 50, 52; fig. 4.AH.

Material. 41 elements: 13 P, 8 Sa, 1 Sb, 1 Sc, 2 Sd, 16 Sc (CORD-MP 8049/1, 8057/1–2, 8097/1–2, 8123/1–3, 8132/1–3, 16501/1–16, 16591/1–2, 16603/1–7, 16624/1, 16708/1–4).

Holotype. P element, CORD-MP 16501/1 (Figure 7V);

Paratype. P element, CORD-MP 16501/7 (Figure 9AC).

Derivatio nominis. After Gondwana, the supercontinent to which the Central Andean Basin formed a part of during the Cambrian–Ordovician periods.

Type locality and stratotype. Huacalera, Tilcara Department, Jujuy Province, Argentina. El Arenal section, level ElArB, *ca*. 8 m above the base of the Rupasca Member, Santa Rosita Formation (Figure 3).

Diagnosis. New species of *Kallidontus* Pyle and Barnes including non-geniculate and platform morphotypes, where the coniform elements are laterally compressed having one or two keeled processes and the platform elements are carminiscaphate, antero-posteriorly compressed, with two to four lateral keels and a concave posterior margin. All elements are proclined and present soft rings of crests, parallel to the base, and incipient small nodes on the processes.

Description. The elements show wide bases, slender walls and deep basal cavities. The presence of basal filling is frequent (Figures 9AE, AG, AH). The ornamentation consists of conspicuous crests parallel to the base.

The diagnostic P element is symmetric, it is antero-posteriorly compressed, having the posterior flank concave and the anterior convex. Two keels extend along the lateral margins, with small nodes (Figure 9AC). The ratio length/width of the element is over 1, the cusp is poorly developed and tapers to a stout tip. The basal margin is suboval. A juvenile P element has two antero-lateral processes, two postero-lateral processes and the basal margin is quadrangular.

The Sa (symmetrical) element is laterally compressed, with a keel in the posterior margin and a rounded anterior margin (Figures 7W and 9AD).

The Sb element has a flat antero-lateral flank, bounded by anterior and antero-lateral carinae on the outer-lateral flank outlining an asymmetrical appearance.

The anterior and posterior margins of the subsymmetrical Sc element are keeled, and it is laterally compressed. The cusp is the less proclined of all of the morphotypes of the species apparatus.

The Sd element is similar to the Sb but it presents more rectilinear anterior and posterior margins, and the outer lateral flank developes like a costa, which is located in a medial position.

The elements are ornamented by crests or growth lines parallel to the oral margin, which give a terraced aspect to the element surface. The basal cavity is deep, almost reaching the apex of the cusp. The walls of the element are thin, slightly folded and rough.

Discussion. The observed characteristics of recorded elements coincide with the new genus created by Pyle and Barnes (2002), including P (platform) and S (coniform symmetry transition series) elements. The differentiation of the S series morphotypes is provisional until new material is collected.

Kallidontus gondwanicus n. sp. is distinguished from the forms originally described by Pyle and Barnes (*K. serratus*, *K. nodosus* and *K. princeps*) by a poor ornamentation of crests and nodes, small size and simple design. This species is a possible ancestor of *K. princeps* Pyle and Barnes, 2002 given that this taxon is recorded in younger successions of the Parcha area, in the Cordillera Oriental (Albanesi *et al*., 2007a, 2008). The P element of *K. gondwanicus* differs from the P element of *K. princeps* by being longer and symmetrical.

This new species has been also determined from a new conodont collection of the Tiñú Formation (Oaxaca, México), which is incorporated for taxonomic comparison (Figure 9AE, AH).

Occurrence and age. Alfarcito and Rupasca members, Santa Rosita Formation, and Lower Member, Coquena Formation. *Cordylodus angulatus* Zone–*Paltodus deltifer* Zone, early Tremadocian (Tr1)–middle Tremadocian (Tr2), Early Ordovician.

Order PROTOPANDERODONTIDA Sweet, 1988
Family ACANTHODONTIDAE Lindström, 1970
Genus *Acanthodus* Furnish, 1938

?1980. *Monocostodus* Miller: 26, 27.

Type species. *Acanthodus uncinatus* Furnish, 1938, original designation.

Emended diagnosis. Seximembrate apparatus that consists of a symmetry transition series of acanthodiform (Sb–Sc–Sd), drepanodiform (M), scandodiform (P), and suberectiform elements (Sa), where each morphotype has a variable inclination within a certain range. The surface may be smooth or with microstriae, especially in the rear flank. The posterior margin of the cusp is keeled and its anterior margin is rounded (or keeled in some species).

Remarks. Some species may have small serration on the posterior margin of the cusp (e.g. *Acanthodus uncinatus*) which is not diagnostic at the generic level. Furnish (1938) pointed out that 'all of the syntypes (of *A. uncinatus*) are moderately large; smaller specimens may not show denticles. The prominence of the denticulations shows some variation within the species'. Druce and Jones (1971) illustrated specimens of *A. costatus* Druce and Jones with different sizes of the denticles, and Ji and Barnes (1994) omitted this feature in their emended diagnosis of the genus. In fact, these latter authors did not find serrations in some elements of *A. lineatus* (Furnish, 1938) and *A. uncinatus*.

Discussion. Landing *et al*. (1996) proposed an emended diagnosis for *Acanthodus* Furnish, including the possible

presence of microstriae on the surface of the elements. Based on the collection studied here, we can distinguish six morphotypes: M, P, Sa, Sb, Sc and Sd. *Drepanodus lineatus* Furnish, 1938 is included within *Acanthodus*, following the opinion of the majority of authors that have described it, so that it does not correspond to the genus *Variabiloconus* Landing *et al*. (1986), as considered by Landing *et al*. (1996). The latter taxon has more robust elements, with large bases and the presence of subordinate keels.

Miller (1980) created the genus *Monocostodus* including 'slender, erect to reclined, simple cones; dextral, sinistral and rare bilaterally symmetrical variants produced by changes in the position of narrow, sharp costa beginning near the cusp curvature and extending to tip; costa usually on right or left side, rarely posterior. Cross section of base and lower cusp round to oval; cusp composed of white matter'. The characteristics described by Miller for *Monocostodus* match those of the genus *Acanthodus* Furnish, in the emended diagnosis that arises in this work, except that *Monocostodus* in its monotypic species, *M. sevierensis* (Miller, 1969) seems to have a simple apparatus, consisting of only two morphotypes, although more morphotypes could be present in this yet poorly known species. Until new evidences appear, we suggest a possible synonymy for these two taxa.

The proposed emended diagnosis in this study highlights the variability in the inclination of the cusp with respect to the oral margin in each morphotype. This feature is also observed by Serpagli *et al*. (2008) in the species *Teridontus gallicus* Serpagli *et al*., 2008, where each morphotype has a variable inclination range while retaining the shape of the contour of the base. Following the emended diagnosis of the genus *Teridontus* by those authors, the diagnostic characters of *Acanthodus* are the contour of the base and the angle between the major axis of the base and the axis of the cusp.

Fahraeus and Roy (1993) illustrated specimens of *A. lineatus* with an architectural plan similar to that of the new species described herein; figs. 1–6 of plate 1 (op. cit.) corresponds to the morphotypes Sc, M, Sb, Sa, M and P, respectively, of *A. lineatus*).

Acanthodus humachensis n. sp.
Figures 7H–N, 9P–AB

Material. 72 M element, 44 P elements, 58 Sa elements, 32 Sb elements, 45 Sc elements, 50 Sd elements (CORD-MP 16638/1–265, 16654/1–22, 16668/1–4).

Holotype. P element, CORD-MP 16638/64 (Figure 7I);

Paratype. P element, CORD-MP 16638/103 (Figure 9S).

Derivatio nominis. Referring to the locality Humacha, near the city of Huacalera, where the holotype of this new species comes from.

Type locality and stratotype. Huacalera, Tilcara Department, Jujuy Province, Argentina. Humacha section, level Hum1, *ca*. 38.50 m above the base of the Humacha Member, Santa Rosita Formation (Figure 4).

Diagnosis. An *Acanthodus* species that consists of elongate elements, short bases in relation to the cusp, keeled anterior and posterior margins, without serration, and surface with microstriae. The outer flank bears a costa on the base, which disappears into the cusp.

Description. M element: suberect to slightly proclined cusp, with a marked furrow or depression on antero-lateral position (Figure 9P). Some specimens show the antero-basal angle projected downwards. Triangular basal profile.

P element: short base, suberect to slightly proclined cusp, with a costa on the outer flank that originates near the aboral margin and becomes faint to the cusp (Figures 7I–J, 9T). The element presents a strong lateral compression.

Sa element: symmetrical morphotype, with basal subcircular to oval contour, and slightly proclined cusp. The anterior margin of the cusp is keeled but the anterior margin of the base is smooth. The keel of the posterior margin of the cusp can continue to the oral margin.

Sb element: longer base than in the other morphotypes, and strongly proclined cusp. A weak costa is present close to the anterior margin, and the element is bilaterally compressed.

Sc element: short base, subtrapezoidal basal contour due to an additional costa on the inner flank close to the anterior margin of the base. An imaginary line drawn down the posterior margin of the cusp intersects near the antero-basal angle, while the oral margin extends posteriorly.

Sd element: wide base, subquadrangular contour, similar to the Sc morphotype, but with longer base due the antero-basal angle and the oral margin are projected posteriorly.

The morphotypes present microstriae although faint (Figure 9U) and in some specimens the keels tend to become thin laminae, particularly on the posterior margin (Figure 9W). The walls are thick, because of which it is not possible to observe the basal cavity generally.

Discussion. Acanthodus humachensis n. sp. differs from *A. lineatus* (Furnish) and *A. costatus* by having short-weak costae, which do not extend into the cusp. *A. uncinatus* presents Sa erectiform element that differs from the species described herein, whose Sa morphotype has teridontiform with proclined cusp.

Occurrence and age. Humacha Member, Santa Rosita Formation, and Upper Member, Coquena Formation. *Paltodus deltifer* Zone (*Paltodus deltifer deltifer* Subzone), middle Tremadocian (Tr2), Early Ordovician.

Acanthodus raqueli n. sp.
Figures 7A–G, 9A–O

1998. *Monocostodus sevierensis* (Miller). Rao and Tortello: 36; pl.1:13–18, fig. 3.

2000. *Monocostodus sevierensis* (Miller). Tortello and Rao: 78–79; figs. 5.D, E, G, I, K, L.

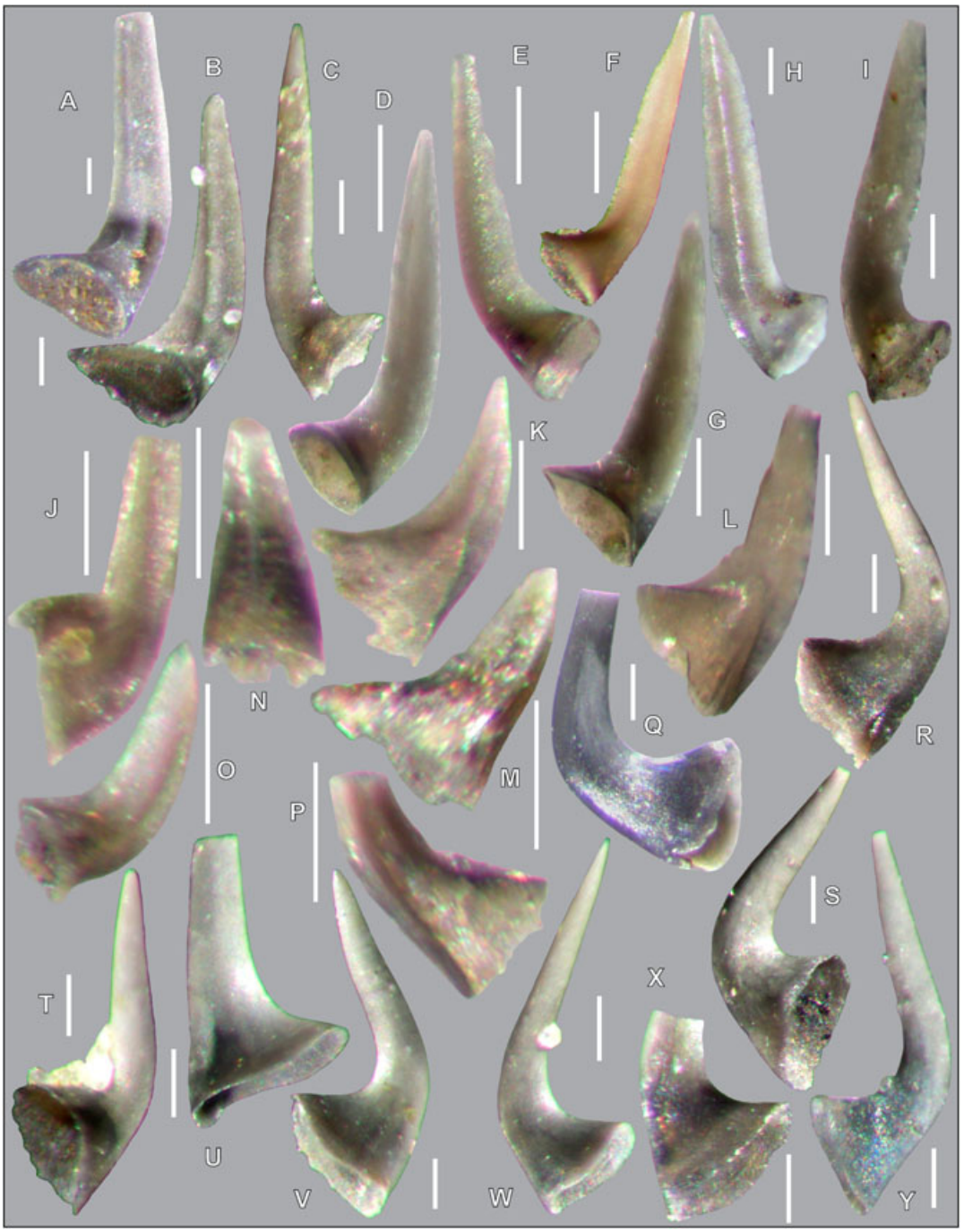

Figure 6. (A–C) *Utahconus tortibasis* n. sp., (A, B) M elements, postero-lateral views (**holotype:** CORD-MP 16479/1, sample CC4, CORD-MP 12497/1, sample ElArA); (C) P element, inner lateral view (CORDMP 16479/387, sample ElArA). (D–F) *Utahconus purmamarcensis* n. sp., (D) M element, postero-lateral view (**holotype:** CORD-MP 11306/1, sample CoqSup); (E, F) P elements, inner lateral views (CORD-MP 16615/13, sample Chal1, CORD-MP 16586/32, sample CoqSup). (G–I) *Utahconus scandodiformis* n. sp., (G) M element, postero-lateral view (**holotype:** CORD-MP 11304/1); (H, I) P elements, inner lateral view (CORD-MP 16653/23, CORD-MP 11305/1) (all specimens from sample Hum2). (J–P) *Acodus primitivus* n. sp., (J) M element, inner lateral view (CORD-MP 16655/11); (K) Pa element (early form), outer lateral view (**holotype:** CORD-MP 16635/7); (L) Pa element (late form), outer lateral view (CORD-MP 16655/3); (M) Pb element, outer lateral view (CORD-MP 16635/21); (N) Sa element, posterior view (CORD-MP 16635/1); (O) Sb element, inner lateral view (CORD-MP 16635/2); (P) Sc element, inner lateral view (CORD-MP 16635/34) (all specimens from sample Hum1, except K and M from sample Hum2). (Q–Y) *Variabiloconus crassus* n. sp., (Q, R) M element, inner lateral views (CORD-MP 16699/1, CORD-MP 16480/1); (S) Pa1 element, outer lateral view (CORD-MP 16480/97); (T) Pa2 element, outer lateral view (**holotype:** CORD-MP 16480/116); (U) Sa element, lateral view (CORD-MP 16480/135); (V) Sb element, inner lateral view (CORD-MP 16480/148); (W) Sc element, inner lateral view (CORD-MP 16480/171); (X) Pb element, inner lateral view (CORD-MP 16480/232); (Y) Sd element, outer lateral view (CORD-MP 16480/232) (all specimens from sample ElArA, except Q from Tramp3). A–C, Q–Y specimens occur in the *Cordylodus angulatus* Zone, D–F specimens occur in the *Paltodus deltifer pristinus* Subzone, and G–P specimens occur in the *Paltodus deltifer deltifer* Subzone. Scale bar: 0.1 mm. This figure is available in colour online at wileyonlinelibrary.com/journal/gj

Figure 7. (A–G) *Acanthodus raqueli* n. sp., (A, B) M elements, inner lateral views (CORD-MP 16486/1, CORDMP 16486/2); (C) P element, inner lateral view (**holotype:** CORD-MP 16486/13); (D) Sa element, postero-lateral view (CORD-MP 16486/184); (E) Sb element, inner lateral view (CORD-MP 16486/252); (F) Sc element, inner lateral view (CORD-MP 16486/349); (G) Sd element, inner lateral view (CORD-MP 16486/427) (all specimens from sample ElArA). (H–N) *Acanthodus humachensis* n. sp., (H) M element, inner lateral view (CORD-MP 16654/1); (I, J) P elements, outer lateral views (**holotype:** CORD-MP 16638/64, CORD-MP 16638/65); (K) Sa element, lateral view (CORD-MP 16638/105); (L) Sb element, outer lateral view (CORD-MP 16638/156); (M) Sc element, outer lateral view (CORD-MP 16638/187); (N) Sd element, outer lateral view (CORD-MP 16638/230) (all specimens from sample Hum1, except H from sample Hum2). (O–U) *Tilcarodus humahuacensis* (Albanesi and Aceñolaza) (late form), (O) M element, inner lateral view (CORD-MP 16498/1); (P) Pa element, postero-lateral view (**paratype:** CORD-MP 16498/44); (Q) Pb element, postero-lateral view (CORD-MP 16498/145); (R) Sa element, posterior view (CORD-MP 16498/184); (S) Sb element, postero-lateral view (CORD-MP 16498/209); (T) Sc element, posterior view (CORDMP 16498/277); (U) Sd element, inner lateral view (CORD-MP 16498/349) (all specimens from sample ElArB). (V–Z) *Kallidontus gondwanicus* n. sp., (V) P element, posterior view (**holotype:** CORD-MP 16501/1); (W) Sa element, lateral view (CORD-MP 16501/8); (X) Sb element, inner lateral view (CORD-MP 16501/11); (Y) Sc element, lateral view (CORD-MP 16501/12); (Z) Sd element, outer lateral view (CORD-MP 16501/16) (all specimens from sample ElArB). A–G, V–Z specimens occur in the *Cordylodus angulatus* Zone, O–U specimens occur in the *Paltodus deltifer pristinus* Subzone, and H–N specimens occur in the *Paltodus deltifer deltifer* Subzone. Scale bar: 0.1 mm. This figure is available in colour online at wileyonlinelibrary.com/journal/gj

2008. *Teridontus gracillimus* Nowlan. Zeballo *et al*.: fig. 4.16.

Material. 150 M elements, 137 P elements, 105 Sa elements, 123 Sb elements, 104 Sc elements, 104 Sd elements. (CORD-MP 8007/1–2, 8042/1–49, 11307/1, 16486/1–505, 16518/1–14, 16570/1–32, 16585/1–49, 16598/1–5, 16617/1–47, 16670/1, 16693/1–18).

Holotype. P element, CORD-MP 16486/13 (Figure 7C);

Paratype. P element, CORD-MP 16486/146 (Figure 9E).

Derivatio nominis. In tribute to Dr Raquel I. Rao, who described elements of this species for the first time and pioneered the study of conodont faunas from the Cordillera Oriental of Argentina.

Type locality and stratotype. Huacalera, Tilcara Department, Jujuy Province, Argentina. El Arenal section, level ElArA, *ca*. 168 m above the base of the Alfarcito Member, Santa Rosita Formation (Figure 3).

Diagnosis. Species of *Acanthodus* with elongate morphotypes, straight cusp of variable inclination (from proclined to erect to reclined), without serration, with keeled posterior margin, rounded anterior margin, short base and surface with microstriae. The keel that extends along the posterior margin of the cusp is frequently torsioned with respect to the sagital plane of the element.

Description. M element: this element presents a shallow furrow adjacent to the acute anterior margin. The cusp is suberect to slightly reclined. The basal contour is suboval with a flat inner side and a rounded outer side, whose axis coincides with the axis of the cusp.

P element: the base is short, with subcircular contour and a strongly proclined cusp (Figure 7C). The axis of the basal contour differs from the axis of the cusp in an angle lower than 10° (Figure 9F).

Sa element: symmetrical element with suberect to weakly proclined cusp. The base is long with oval contour and an axis perpendicular to the axis of the cusp.

Sb element: strongly asymmetrical morphotype, of long bilaterally compressed base, and deflected with respect to the plane of the cusp, which is slightly proclined. The contour of the base is oval compressed and its axis forms an angle over 10° with respect to the axis of the cusp (Figure 9K).

Sc element: subsymmetrical morphotype, with short base and weak carinae on antero-basal position that delineates a subrectangular to suboval contour. The axis between the base and the cusp is less than 10° with the cusp, which is slightly proclined and reclined.

Sd element: this form is similar to the Sc morphotype but with a more expanded base posteriorly, of triangular profile, and the ratio cusp/basal length is lower. Some elements present a small depression in the posterior margin, associated to two weak costae in the transitional base to cusp space.

All morphotypes exhibit microstriae, which are more prominent in the transitional zone between the base and the cusp (Figure 9B). The posterior margin of the cusp is keeled. This keel is frequently deflected towards the upper cusp (Figure 9F, M), except for the morphotypes M and Sa. The elements are completely albid, with higher concentration of white matter in the upper part of the cusp, while in the base its presence is fuzzy. The basal cavity is deep, with triangular profile and its tip is located nearby the anterior margin. The adult specimens differ from the juveniles by wider expansion of the base to posterior and a more divergent oral margin with respect to the antero-basal margin.

In *A. raqueli* n. sp. the inclination of the cusp together with the form and size of the base are the typical characters that differentiate the species morphotypes. However, the inclination of the cusp in a morphotype is variable within a discrete range.

Discussion. Rao and Tortello (1998) illustrated and described in detail material from the Incamayo Creek, Incahuasi area (Salta Province, *ca*. 120 km to south of the study area, Figure 1) assigning it to *Monocostodus sevierensis*. This material is an association virtually identical to the levels recorded in the contemporary *Cordylodus angulatus* Zone of the area studied in this work. *Monocostodus sevierensis* has a shallower basal cavity and its apex is closer to the posterior margin than to the anterior margin. Moreover, it is restricted to the later Cambrian *Cordylodus intermedius* Zone. Therefore, the determination made by Rao and Tortello (1998) is incorrect, and the material in question is reassigned to *Acanthodus raqueli* n. sp.

Acanthodus lineatus is the species closest to *A. raqueli* n. sp., differing from the latter by the presence of a groove and associated costa in the antero-lateral margin of the cusp of all morphotypes. Moreover, *A. raqueli* n. sp. presents a structural plan similar to that of *A. humachensis* n. sp., although the latter presents the anterior and posterior margins of the cusp keeled and has lateral costae. Both taxa could be phylogenetically related, with *A. raqueli* n. sp. being the ancestor of *A. humachensis* n. sp.

Occurrence and age. Alfarcito and Rupasca members, Santa Rosita Formation, Lower Member, Coquena Formation, and Devendeus Formation. *Cordylodus angulatus* Zone–*Paltodus deltifer* Zone (*P. d. pristinus* and *P. d. deltifer* subzones), early Tremadocian (Tr1)–middle Tremadocian (Tr2), Early Ordovician.

Geographic and stratigraphic distribution. Argentina (Rao and Tortello, 1998). *Cordylodus angulatus* Zone, early Tremadocian (Tr1), Early Ordovician.

Family ONEOTODONTIDAE Miller, 1980
Genus *Utahconus* Miller, 1980

Type species. Paltodus utahensis Miller, 1969, original designation.

Discussion. Zeballo *et al*. (2005b) and Albanesi and Aceñolaza (2005) proposed a revised diagnosis for the genus *Utahconus*, which possess a quinquimembrate apparatus of

elements along with elements of modified pyramidal shape. The species *Utahconus humahuacensis* Albanesi and Aceñolaza, 2005 (= *Utahconus* n. sp. Zeballo *et al*., 2005b) can not be referred to *Utahconus* as it develops a more complex apparatus, which is septimembrate with triangulariform elements; therefore, it is reassigned to a new genus (see discussion of *Tilcarodus* n. gen.). Therefore, the diagnosis is accepted as emended by Pyle and Barnes (2002), where the apparatus design is simple, tri- to quadrimembrate and species would fit properly as described below, along with the type species *U. utahensis* (Miller, 1969). In turn, Landing *et al*. (1996), Landing *et al*. (2003), and Tolmacheva and Abaimova (2009) synonymized *Utahconus* with *Scalpellodus* Dzik, using the first genus mentioned by nomenclatural priority. However, *Scalpellodus* elements have different characteristics, and they are of later development (Middle Ordovician), since the genus *Utahconus* is considered valid to designate the forms restricted to the Furongian to Early Ordovician.

Multielement apparatuses described below present an M element, which in this work is assigned to the bicostate element, an S element, and a P element that would be equivalent to the unicostate element of *Utahconus*, as interpreted by Miller (1980). The lack of the Sa morphotype in some described species may be due to the loss of such a form in the multi-element apparatus of the taxa described herein, or a population sampling problem, since when the Sa element is present in other species, it appears in a lesser frequency than other morphotypes. Ji and Barnes (1994) pointed out that the c element (= Sa) may be rare or absent in early species of this genus.

Utahconus purmamarcensis n. sp.
Figures 6D–F, 8H–M

2008. *Utahconus longipinnatus* Ji and Barnes. Zeballo *et al*.: fig. 4.15.

Material. 119 elements, among M, P and S elements (CORD-MP 11306/1, 16586/1–73, 16596/1–13, 16615/1–33).

Holotype. Non-geniculate M element, CORD-MP 11306/1 (Figure 6D);

Paratype. Non-geniculate M element, CORD-MP 16586/15 (Figure 8I).

Derivatio nominis. After Purmamarca, the town near the Coquena Creek, where the holotype of the species was found.

Type locality and stratotype. Purmamarca, Tumbaya Department, Jujuy Province, Argentina. Coquena section, level CoqSup, *ca*. 11.75 m below the top of the Lower Member, Coquena Formation (Figure 5).

Diagnosis. *Utahconus* species with three morphotypes: M, asymmetrical, with suberect to slightly proclined cusp, keeled posterior margin and acute rounded margin, S, asymmetrical, with more straight antero-lateral margin and shorter base than M element, and P, subsymmetrical with posterior keel and strongly proclined cusp. Elements present an oval basal contour and flanks without carinae.

Description. This *Utahconus* species presents a simple multielemental apparatus, composed of three morphotypes, M, S and P, with moderate differences within each form in an intraspecific variation range.

M element: asymmetrical element, long base, oval contour and suberect to slightly proclined cusp, which is torsioned with respect to the base, so the basal cavity is located to the inner and posterior flank (Figures 6A–B, 8H–I). The postero-lateral margin of the cusp is keeled and the antero-lateral margin is rounded, not becoming a keel. Surface without ornamental characters. The projection of the postero-lateral margin crosses the antero-basal angle.

S element: asymmetrical element, shorter base and more straight antero-lateral margin than M element. The projection of the postero-lateral margin crosses the basal margin near the middle (Figure 8J).

P element: subsymmetrical element of short base, oval contour and cusp strongly proclined, although there are also some elements with lower angle (Figures 6E–F, 8K–M). The element is bilaterally compressed, the posterior margin is keeled, and the outer flank is smoothly convex.

Discussion. The forms mentioned by Pyle and Barnes (2002, 72, pl. 17, figs 1–3) as *U. longipinnatus* Ji and Barnes, 1994 do not correspond to this taxon, since it has less curved anterior and posterior margins and plane inner lateral flank. The illustrated material may belong to a form related to *U. purmamarcensis* n. sp. although the photographed element (op. cit., pl. 17, fig. 1) shows a much stronger posterior keel even becoming a sheet. Identical observations can be made for the material described as *U. longipinnatus* by Agematsu *et al*. (2008, p. 1450, pl. 1, figs 8–10).

Occurrence and age. Lower Member, Coquena Formation. *Paltodus deltifer* Zone (*P. d. pristinus* and *P. d. deltifer* subzones), middle Tremadocian (Tr2), Lower Ordovician.

Utahconus scandodiformis n. sp.
Figures 6G–I, 8N–R

2008. *Protopanderodus inconstans* (Branson and Mehl). Zeballo *et al*.: fig. 4.13.

2008. *Protopanderodus prolatus* Ji and Barnes. Zeballo *et al*.: fig. 4.14.

?1998. *Utahconus* sp. Rao and Flores: 18; pl. 2, fig. 8.

Material. 447 elements, among M, P and S elements (CORD-MP 16606/1–40, 16634/1–347, 16653/1–56, 16667/1–4).

Holotype. Scandodiform M element, CORD-MP 11304/1 (Figure 6G);

Paratype. Scandodiform M element, CORD-MP 16653/21 (Figure 8N).

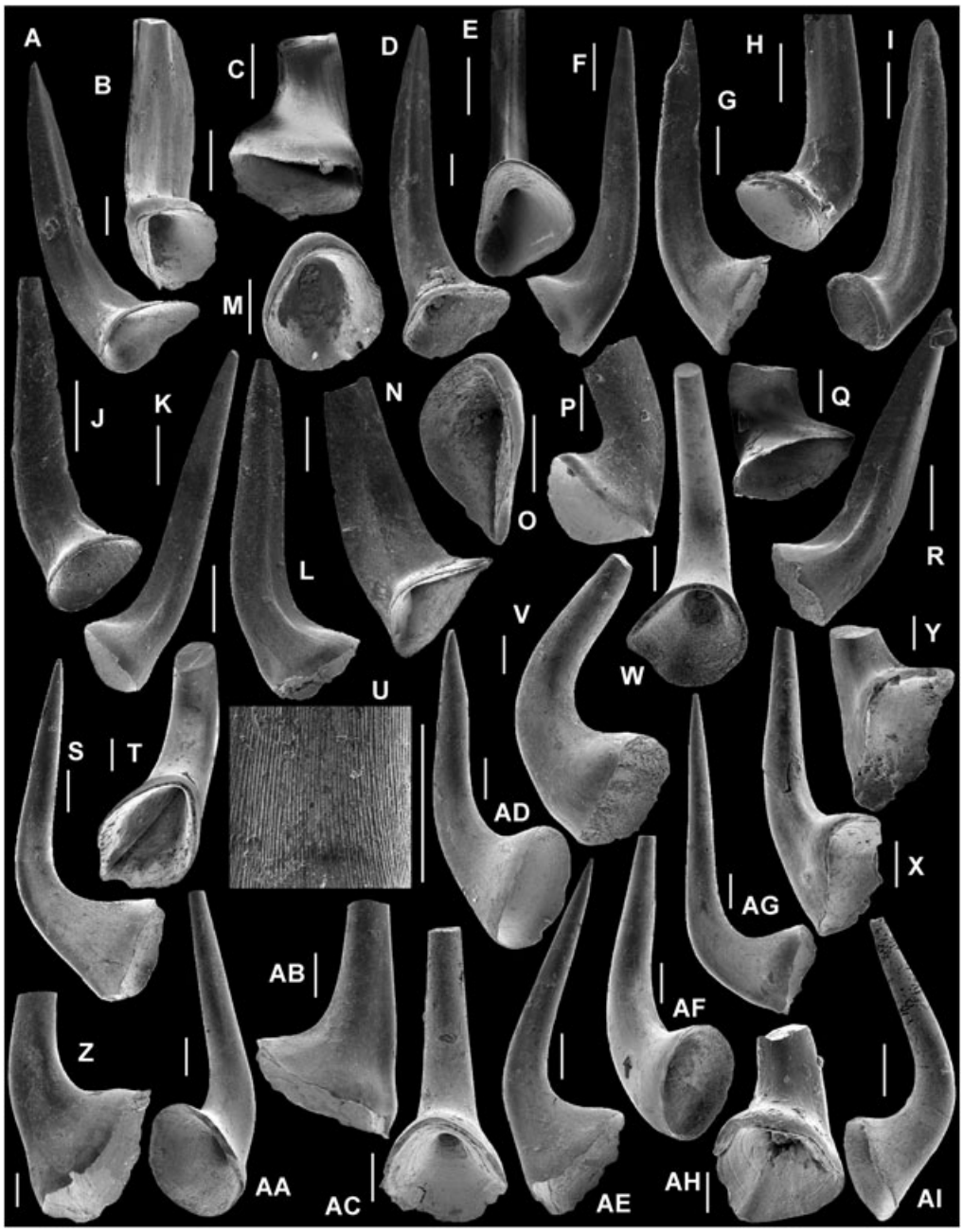

Figure 8. (A–G) *Utahconus tortibasis* n. sp., (A, B) M elements, postero-lateral and basal views (**paratype:** CORD-MP 16479/40, CORD-MP 16479/41); (C) Sa element, posterior view (CORD-MP CORD-MP 8029/1); (D) S element, postero-lateral view (CORD-MP 16479/325); (E–G) P elements, postero-basal and outer lateral views (CORD-MP 16479/420, CORD-MP 16479/421, CORD-MP 16479/422) (all specimens from sample ElArA, except C from sample CC4). (H–M) *Utahconus purmamarcensis* n. sp., (H, I) M elements, postero-lateral views (CORD-MP 16586/14, **paratype:** CORD-MP 16586/15), (J) S element, postero-lateral view (CORD-MP 16586/30); (K–M) P elements, outer lateral and basal views (CORD-MP 16586/52, CORD-MP 16586/53, CORD-MP 16586/54) (all specimens from sample CoqSup). (N–R) *Utahconus scandodiformis* n. sp., (N, O) M elements, postero-lateral and basal views (**paratype:** CORD-MP 16653/21, CORD-MP 16653/22); (P, R) P elements, inner and outer lateral views (CORD-MP 16653/56, CORD-MP 16634/202); (Q) S element, postero-lateral view (CORD-MP 16634/104) (all specimens from sample Hum2, except Q and R from sample Hum1). (S–AI) *Variabiloconus crassus* n. sp., (S–U) M elements, inner lateral, postero-basal views and detail of microstriae on the cusp (CORD-MP 16507/17, CORD-MP 16480/23, and same specimen as in 7S, respectively); (V, W) Pa1 elements, outer lateral and postero-basal views (CORD-MP 16480/10, CORD-MP 16480/11); (X, Y) Pa2 elements, inner lateral views (**paratype:** CORD-MP 8047/39, CORD-MP 8047/40); (Z, AA) Pb elements, inner lateral and postero-lateral views (CORD-MP 8047/49, CORD-MP 16480/238); (AB, AC) Sa elements, lateral and postero-basal views (CORD-MP 8084/64, CORD-MP 16480/147); (AD, AE) Sb elements, postero-lateral and inner lateral views (CORD-MP 16480/170, CORD-MP 16507/34); (AF, AG) Sc elements, postero-lateral and inner lateral views (CORD-MP 16480/146, CORD-MP 16480/147); (AH, AI) Sd elements, postero-basal and inner lateral views (CORD-MP 8047/93, CORD-MP 16480/218) (all specimens from sample ElArA, except X–Z, AB and AH from sample CC8, and S and AE from sample ElArB). A–G, T, V, W, AA, AC, AD, AF, AG, AI specimens occur in the *Cordylodus angulatus* Zone, H–M, S, X–Z, AB, AE, AH specimens occur in the *Paltodus deltifer pristinus* Subzone, and N–R specimens occur in the *Paltodus deltifer deltifer* Subzone. Scale bar: 0.1 mm.

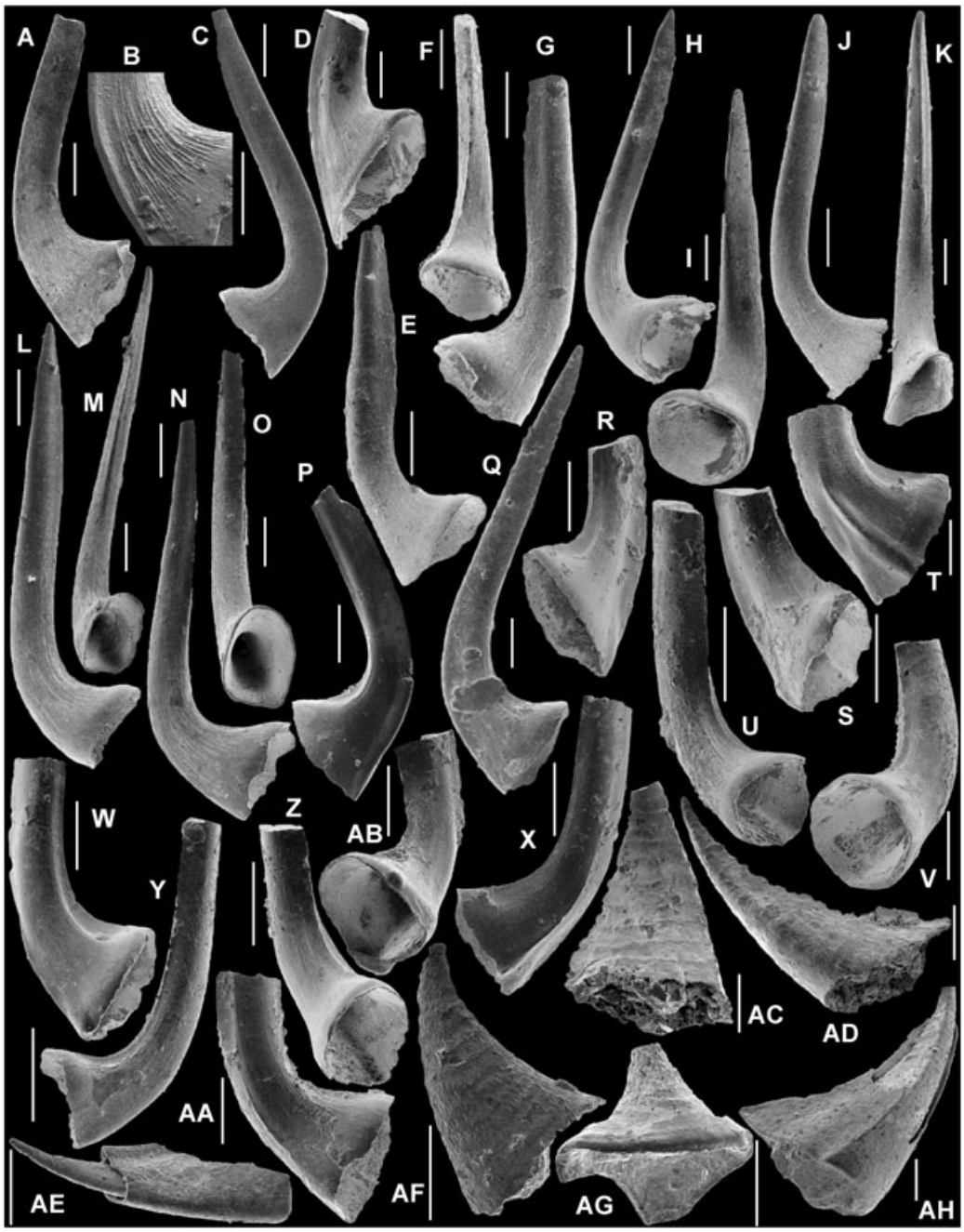

Figure 9. (A–O) *Acanthodus raqueli* n. sp., (A–D) M elements, inner lateral views, detail of microstriae on the surface and postero-basal view (CORD-MP 16486/52, same specimen as in 8A, CORD-MP 16486/53, CORD-MP 16486/54); (E–G) P elements, inner lateral and postero-basal views (**paratype:** CORD-MP 16486/146, CORD-MP 16486-147, CORD-MP 16486/148); (H, I) Sa elements, lateral and postero-basal views (CORD-MP 16486/217, CORD-MP 16486/218); (J, K) Sb elements, inner lateral and postero-basal views (CORD-MP 16486/302, CORD-MP 16486/303); (L, M) Sc elements, inner lateral and postero-basal views (CORD-MP 16486/382, CORD-MP 16486/383); (N, O) Sd elements, inner lateral and postero-basal views (CORD-MP 16486/451, CORD-MP 16486/452) (all specimens from sample ElArA). (P–AB) *Acanthodus humachensis* n. sp., (P–R) M elements, inner lateral and postero-lateral views (CORD-MP 16638/30, CORD-MP 16638/31, CORD-MP 16638/32); (S, T) P elements, postero-lateral and outer lateral views (CORD-MP 16638/103, **paratype:** CORD-MP 16638/104); (U, V) Sa elements, postero-lateral views (CORD-MP 16638/135, CORD-MP 16638/136); (W, X) Sb elements, inner lateral and outer lateral views (CORD-MP 16638/186, CORD-MP 16654/16); (Y, Z) Sc elements, inner lateral and postero-basal views (CORD-MP 16638/206, CORD-MP 16638/207); (AA, AB) Sd elements, outer lateral and postero-basal views (CORD-MP 16638/239, CORD-MP 16638/240) (all specimens from sample Hum1, except X from sample Hum2). (AC–AH) *Kallidontus gondwanicus* n. sp., (AC, AG) P elements, posterior views (**paratype:** CORD-MP 16501/7, sample ElArB, CORD-MP 8097/2, sample SG7B); (AD, AE) Sa elements, lateral views (CORD-MP 16501/10, sample ElArB, CORD-MP 16716/1, sample Tiñú); (AF) Sc element, lateral view (CORD-MP 16624/1, sample Chal1); (AH) Sd? element, lateral view (CORD-MP 16716/3, sample Tiñú). A–O specimens occur in the *Cordylodus angulatus* Zone, AC, AD, AF, AG specimens occur in the *Paltodus deltifer pristinus* Subzone, and P–AB specimens occur in the *Paltodus deltifer deltifer* Subzone. Scale bar: 0.1 mm.

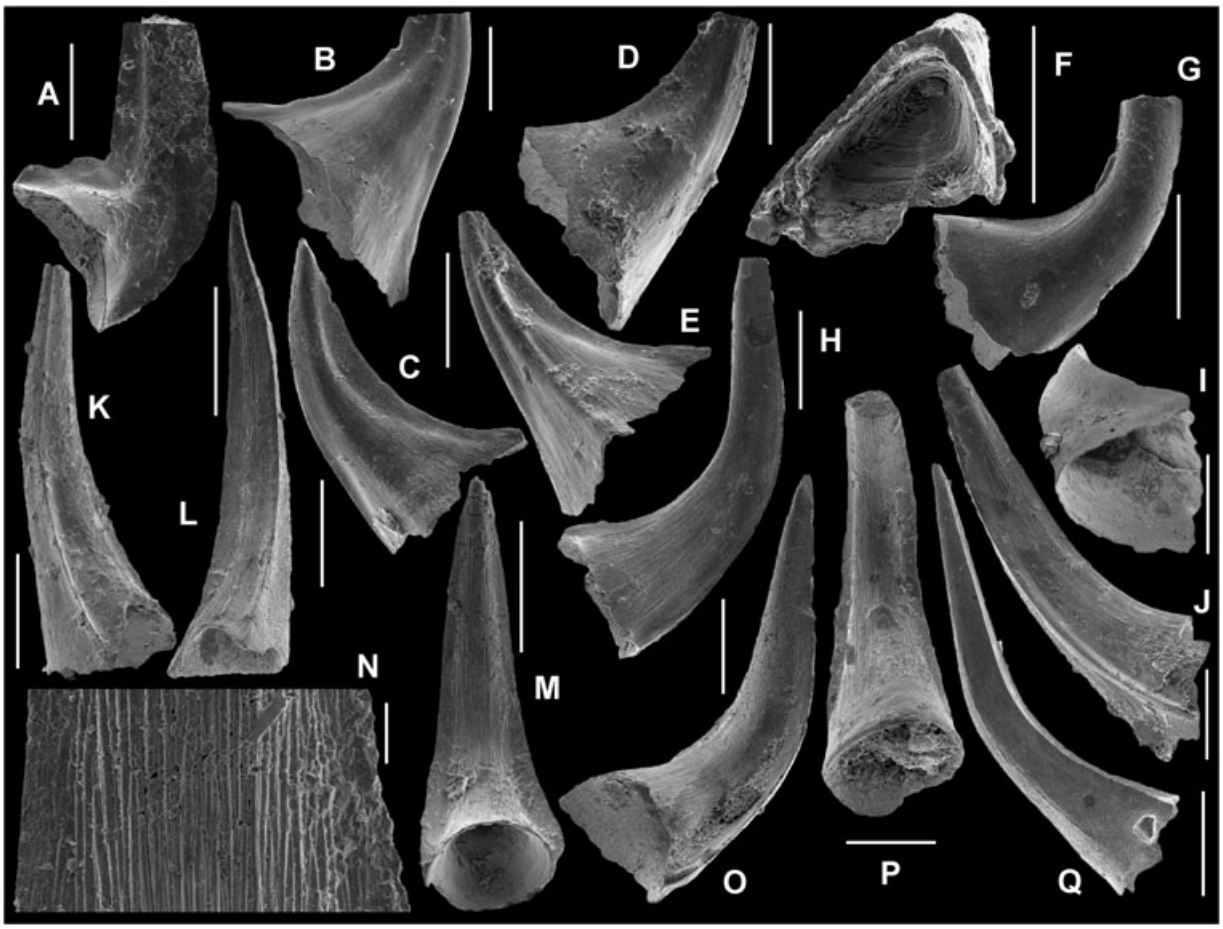

Figure 10. (A–G) *Acodus primitivus* n. sp., (A) M element, inner lateral view (CORD-MP 16655/2); (B–D) Pa elements, outer lateral views (CORD-MP 16635/18, **paratype:** CORD-MP 16635/19, CORD-MP 16635/20); (E, F) Pb elements, outer lateral and basal views (CORD-MP 16635/32, CORD-MP 16635/33); (G) Sc element, inner lateral view (CORD-MP 16635/34) (all specimens from sample Hum1, except A from sample Hum2). (H–Q) *Tilcarodus humahuacensis* (Albanesi and Aceñolaza), (H) M element, inner lateral view (CORD-MP 16498/43); (I, J) Pa elements, basal and postero-lateral view (CORD-MP 16498/143, CORD-MP 16498/144); (K, L) Pb elements, postero-lateral views (CORD-MP 16498/160, CORD-MP 16498/161); (M, N) Sa element, posterior view and detail of microstriae of the same specimen (CORD-MP 16498/208); (O) Sb element, inner lateral view (CORD-MP 16498/240); (P) Sc element, posterior view (CORD-MP 16498/312); (Q) Sd element, outer lateral view (CORD-MP 16498/376) (all specimens from sample ElArB). A–G specimens occur in the *Paltodus deltifer deltifer* Subzone and H–Q specimens occur in the *Paltodus deltifer pristinus* Subzone. Scale bar: 0.1 mm, except N: 0.01 mm.

Derivatio nominis. From the conodont genus *Scandodus*, given the similarity between elements of this species and *Scandodus furnishi* Lindström.

Type locality and stratotype. Huacalera, Tilcara Department, Jujuy Province, Argentina. Humacha section, level Hum2, *ca*. 192 m above the base of the Humacha Member, Santa Rosita Formation (Figure 4).

Diagnosis. Utahconus species of trimembrate multielemental apparatus, whose elements have constrained and short bases, strongly compressed cusps and keeled margins.

Description. The multielemental apparatus of *Utahconus scandodiformis* n. sp. is composed of the M, S and P morphotypes, which do not have ornamentation and are strongly bilaterally compressed.

M element: asymmetrical element with proclined cusp, slightly curved antero-lateral and postero-lateral margins. Similar to other *Utahconus* species, the basal cavity is located to the inner posterior flank. The base is narrow and its contour is roughly ogival (Figure 8O).

S element: similar to M element but its basal contour is more oval (Figure 8Q).

P element: subsymmetrical morphotype, with the inner flank slightly concave and convex outer margin. The cusp can be suberect or weakly reclined (Figure 6I), or proclined (Figure 6H) and presents a weak constraint in its transition to the base, the latter being short with oval contour.

Discussion. Utahconus scandodiformis n. sp. is differentiated from other species described herein, because the anterior and posterior margins are keeled, base short and constrained, and bilaterally compressed. *U. utahensis* presents a continuous curvature through the element, contrary to *U. scandodiformis* n. sp. which exhibits a strong separation between base and cusp.

Occurrence and age. Humacha Member, Santa Rosita Formation, and Upper Member, Coquena Formation. *Paltodus deltifer* Zone (*Paltodus deltifer deltifer* Subzone), middle Tremadocian (Tr2), Early Ordovician.

Utahconus tortibasis n. sp.
Figures 6A–C, 8A–G

1995. *Utahconus utahensis* (Miller). Rao and Hünicken: 258; pl. II, fig. 11, 16; pl. III, fig. 6.
1998. *Utahconus* aff. *longipinnatus* Ji and Barnes. Rao and Tortello: 38; pl. 2: 8–12.
2000. *Utahconus* aff. *longipinnatus* Ji and Barnes. Tortello and Rao: figs. 5.A, B, ?C.
2005b. *Rossodus tenuis* (Miller). Zeballo *et al*.: 62; figs. 3. O–R.
2005. *Rossodus tenuis* (Miller). Albanesi and Aceñolaza: 302, 304; fig. 5.K.
2008. *Utahconus* sp. Albanesi *et al*.: fig. 3.14.

Material. 831 elements, among M, P, S and Sa elements (CORD–MP 8005/1–10, 8014/1–18, 8029/1–89, 8084/1–2, 8099/1–57, 8106/1–22, 16479/1–568, 16513/1–24, 16694/1–41).

Holotype. M element, non-geniculate coniform, CORD-MP16479/1 (Figure 6B);

Paratype. M element, non-geniculate coniform, CORD-MP16479/40 (Figure 8A).

Derivatio nominis. From Latin *torti*: tortioned, and *basis*: base, referring to the asymmetry of the base with respect to the cusp, which develop on different planes.

Type locality and stratotype. Huacalera, Tilcara Department, Jujuy Province, Argentina. El Arenal section, level ElArA, *ca*. 168 m above the base of the Alfarcito Member, Santa Rosita Formation (Figure 3).

Diagnosis. Utahconus species with quadrimembrate multielemental apparatus, with keeled antero-lateral and postero-lateral margins in the M morphotype (bicostate), an oval basal contour in the S element (bicostate), and keeled posterior margin and rounded anterior margin in the P morphotype (unicostate). The forms have a carina associated to one furrow (P element) or two furrows (M and S elements), in the anterior and posterior flanks, respectively. The symmetrical Sa element is rarely recorded and possesses a stout carina in the posterior margin.

Description. M element: suberect to strongly proclined cusp, with a carina close to the inner lateral margin in the apical part and close to the outer lateral margin in the base, which is visible on both the anterior and posterior flanks. The antero-lateral and postero-lateral margins are keeled. The basal contour is ogival; the cusp is torsioned with respect to the base, and is inclined towards one of the flanks (Figure 8B). The basal cavity opens to the inner and posterior flank, and its profile is a scalene triangle with the cusp near the antero-lateral margin. The marked asymmetry of this morphotype is due to the basal cavity and the cusp are twisted and at different levels. The projection of the posterior margin crosses near the antero-basal angle.

Sa element: symmetrical element with a round posterior carina and oval contour of the base (Figure 8C).

S element: asymmetrical element with keeled antero-lateral and postero-lateral margins. The basal contour is more oval than in M element. The projection of the posterior margin crosses at the middle of the oral margin (Figure 8D).

P element: subsymmetrical element, laterally compressed, proclined cusp, but also reclined and suberect specimens. The anterior margin is rounded with a thick carina, and the posterior margin of the cusp has a keel that reaches the oral margin. The base is short and the basal contour is subtriangular–subrounded. The inner lateral flank is weakly concave while the outer flank has a fold in the base and a furrow associated with the anterior carina in the cusp (Figures 8E–G).

All elements present weak microstriae (only discernible with SEM) and the white matter is scattered around the element, but with higher density from the apex of the basal cavity. The strong compression of the cusp in the two morphotypes allows discerning the shape of the basal cavity, since it forms a bulge in the inner flank.

Remarks. Pyle and Barnes (2002) found some variability in the morphotype *e* (= M) of *U. utahensis*. This variability is also observed in the M element of the species described here as they are specimens with more or less asymmetry.

Discussion. Zeballo *et al*. (2005b) and Albanesi and Aceñolaza (2005) described *Rossodus tenuis* (Miller, 1980) from the uppermost strata of the Alfarcito Member and lower Rupasca Member. Close observation of these forms indicates that the material in question does not apply to this genus and should be reassigned to *Utahconus tortibasis* n. sp. The similarities between *Utahconus* Miller and *Rossodus* Ethington and Repetski have caused confusion in previous works of other authors (e.g. Miller, 1980, An *et al*. 1983; Chen and Gong, 1986; Ji and Barnes, 1994). The main difference between the two taxa is that the multielemental apparatus of *Rossodus* is more complex and has geniculate (oistodiforms) elements. *Rossodus tenuis* derived from the *Utahconus* lineage as suggested by Ji and Barnes (1994). These authors described specimens assigned to *Rossodus tenuis*, but because none of the illustrated elements is clearly geniculated, these forms are considered to belong to an *Utahconus* species not yet named.

Utahconus tortibasis n. sp. differs from *U. purmamarcensis* n. sp. by having the basal contour ogival instead of oval in the M element, and a postero-lateral carina. The P element has a carina and a depression on the outer side, the base is shorter and the cusp straighter.

Both *U. tortibasis* as *U. purmamarcensis* have fewer morphotypes compared to ancestral species as it occurs between

U. longipinnatus and *U. utahensis* (cf. Pyle and Barnes, 2002). This reduction could be due to environmental specialization and the consequent loss of some morphotypes in the younger species.

Occurrence and age. Alfarcito and Rupasca members, Santa Rosita Formation, and Devendeus Formation. *Cordylodus angulatus* Zone–*Paltodus deltifer* Zone (*Paltodus deltifer pristinus* Subzone), early Tremadocian (Tr1)–middle Tremadocian (Tr2), Early Ordovician.

Geographic and stratigraphic distribution. Argentina (Rao and Tortello, 1998; Tortello and Rao, 2000; Zeballo *et al*., 2005a, b; Albanesi and Aceñolaza, 2005). *Cordylodus angulatus* Zone, early Tremadocian (Tr1), Early Ordovician.

Family PROTOPANDERODONTIDAE Lindström, 1970
Genus *Variabiloconus* Landing, Barnes and Stevens, 1986

Type species. Paltodus bassleri Furnish, 1938, original designation.

Emended diagnosis. Variabiloconus Landing *et al*. (1986) has a multielemental apparatus that consists of seven non-geniculate morphotypes, showing ornamentation of grooves of varying depth, associated with ribs, carinae and keels. The surface of the elements is microstriated, the cusp is completely albid and the base is hyaline with different amount of white matter. There was an increase of ornamentation and development of the cusp from oldest to youngest taxa.

Variabiloconus crassus n. sp.
Figures 6Q–Y, 8S–AI

?1971. *Oneotodus variabilis* Lindström. Druce and Jones: 84; pl. 13, figs. 5a–c; text–fig. 26 m.
?1971. *Oneotodus variabilis* Lindström. Jones: 60; Pl. 4, figs. 10a–c.
1998. *Teridontus obesus* Ji and Barnes. Rao and Tortello: 37, 38; pl. 2.1–7.
2005b. *Variabiloconus variabilis* (Lindström). Zeballo *et al*.: 60; fig. 4.AF.
2005b. *Teridontus obesus* Ji and Barnes. Zeballo *et al*.: 61; fig. 3.I–L (only).
2008. *Teridontus obesus* Ji and Barnes. Zeballo *et al*.: fig. 4.12.

Material. 262 M elements, 41 Pa1 elements, 52 Pa2 elements, 46 Pb elements, 51 Sa elements, 63 Sb elements, 98 Sc elements, 94 Sd elements, 8 P elements, 38 Pa elements, 7 S elements, 22 elements (CORD-MP 8004/1–13, 8013/1–14, 8040/1–48, 8044/1–7, 8047/1–117, 8075/1–6, 8087/1, 8091/1–35, 8111/1–2, 11303/1, 16466/1–17, 16480/1–238, 16507/1–50, 16517/1–12, 16541/1–7, 16550/1–7, 16556/1–5, 16674/1–44, 16677/1–45, 16681/1–28, 16689/1–11, 16692/1–23, 16699/1–51).

Holotype. Pa2 element, CORD-MP 16480/116 (Figure 6T);
Paratype. Pa2 element, CORD-MP 8047/39 (Figure 8X).

Derivatio nominis. From Latin *crassus*: thick; referred to the large size of the bases and cusps, and the thickness of the walls of the elements.

Type locality and stratotype. Huacalera, Tilcara Department, Jujuy Province, Argentina. El Arenal section, level ElArA, *ca*. 168 m above the base of the Alfarcito Member, Santa Rosita Formation (Figure 3).

Diagnosis. Variabiloconus species with seven morphotypes, thick-walled and robust elements, whose only ornamentation are weak depressions or grooves and carinae. The M element has a shallow groove associated with the acute anterior margin. It is possible to differentiate two Pa morphotypes, one with subcircular basal margin and the other one with subtriangular basal outline, both with a lateral notch. The inner flank of the Pb element is weakly concave and its anterior margin faintly curved. The Sa morphotype is erectiform to proclined and the base of the Sb element has a slight twist with respect to the cusp. The Sc element is subsymmetrical and the Sd element is asymmetrical with long base and four ribs. The cusps are well developed, and are fully albid, but also the basal parts have a variable amount of white matter.

Description. M element: shows lateral compression and a shallow groove associated with acute anterior margin runs along the base to the bottom of the cusp in the inner flank (Figures 6Q and 8S). The aspect of the whole element is gently concave–convex and the cusp is reclined.

Pa1 element: the base is wide and short, with a notch or fold on the outer side (Figure 8W), the cusp is laid back and the basal outline is subcircular.

Pa2 element: the diagnostic form of this species has erect to slightly reclined cusp, base short and broad, subtriangular basal margin and presence of a notch in the outer side (Figure 8Y). Curved anterior margin. The cusps are short compared to the other morphotypes of this species.

Pb element: similar to Pa morphotype except that the inner flank is slightly concave, its anterior margin is weakly curved and has no lateral notch. A faint depression is adjacent to the acute anterior margin.

Sa element: symmetrical morphotype, slightly proclined, short oral margin, antero-basal corner projected below the basal margin, oval basal margin. In the adult stage from younger levels it is possible to see two grooves that delimit fledgling lamellar projections ('wings' sensu Löfgren *et al*., 1999) near the anterior margin, which is rounded or flat (Figures 6U, 8AB).

Sb element: oral margin short, suberect cusp and inner flank gently concave. At younger levels it is possible to see a rib in the posterior margin of the cusp reaching the oral margin. The base shows a slight twist with respect to the cusp, so the element is slightly asymmetrical (Figure 6V, 8AD–AE).

Sc element: biconvex morphotype subsymmetrical or plano-convex. The anterior margin is slightly sharp and is slightly shifted toward the inner edge.

Sd element: the long base and the subtrapezoidal basal outline due to the presence of four ribs of different sizes at the base are characteristics of this form (Figure 6Y and 8AH–AI).

The white matter fills the cusp and is irregularly distributed to the base where it is mixed in the form of threads with the apatite of the base, darker in colour. Elements exhibit slightly sacaroid brightness due to the presence of microstriae that are not discernible with stereomicroscope magnification but only visible with SEM (Figure 8U).

Discussion. The general structure of the multielemental apparatus *Variabiloconus crassus* n. sp. is similar to that of *V. datsonensis* (Druce and Jones, 1971), but there exhibits more differences between the morphotypes, and the cusps are more developed.

Among other distinguishing characteristics, the Pa element of *V. datsonensis* has its antero-basal margin down less prolonged, and the Sa element (symmetrical) of the same taxon has its anterior margin slightly curved posteriorly. *V. variabilis* (Lindström, 1955) and *V. transiapeticus* Löfgren *et al*., 1999 have greater ornamentation of ribs and deeper grooves. *Oneotodus erectus* Druce and Jones, 1971, could correspond to the Sa morphotype of *Variabiloconus crassus* n. sp., but the latter is less proclined. *O. erectus* can bring Sa morphotypes from more than one species, so the material assigned to this taxon needs revision.

Apparently *Variabiloconus crassus* n. sp. evolutionarily derived from *V. datsonensis* and could represent an ancestral form of another more complex species of the genus, such as *V. variabilis* and *V. transiapeticus*. As noted in the emended diagnosis of the genus, the characters observed from *V. datsonensis* and *V. bicuspatus* (Druce and Jones, 1971) to *V. variabilis* show a progressive increase in ornamentation and, in turn, decreased the size of the bases, in their length and in width. Some features, such as the ribs in the Sd elements of *V. crassus* n. sp., are also seen in Sd elements of other *Variabiloconus* species.

V. crassus n. sp. is recorded in the upper part of the *Cordylodus angulatus* Zone and the lower *Paltodus deltifer* Zone. The specimens recovered from upper levels show an ornamentation of grooves and ribs much more profuse, even with the antero-basal margin more expanded in the Pa morphotype, and the basal indentation extends in a gentle carina on the lateral side. The morphotype Pa1 tends to disappear in the younger records being replaced by a progressive increase of the Pa2 morphotype.

Occurrence and age. Alfarcito and Rupasca members, Santa Rosita Formation, and Devendeus Formation. *Cordylodus angulatus* Zone–*Paltodus deltifer* Zone (*Paltodus deltifer pristinus* Subzone), early Tremadocian (Tr1)–middle Tremadocian (Tr2), Early Ordovician.

Geographic and stratigraphic distribution. Argentina (Rao and Tortello, 1998). *Cordylodus angulatus* Zone, early Tremadocian (Tr1), Early Ordovician.

Genus *Tilcarodus* n. gen.

Type species. Utahconus humahuacensis Albanesi and Aceñolaza, 2005, original designation.

Derivatio nominis. Referred to the Tilcara city, Jujuy, and to the homonymous range, where this new genus was recorded.

Diagnosis. Septimembrate apparatus composed of M elements with proclined and laterally compressed cusp; Pa elements with pyramid-shaped cusp, bearing two or three lateral costae, twisted, and triangular basal margin; erectiform Pb elements, with two posterior costae; Sa element, symmetrical, with two lateral keels and proclined cusp; Sb elements similar to morphotype Sa, but postero-laterally compressed, with torsioned cusp; Sc elements subsymmetrical, similar to Sa morphotype but with a half-posterior carina shifted to one of the flanks, and Sd elements, proclined, multicostate, and rounded base. The elements are hyaline, with little white matter concentrated at the top of the cusp; the basal cavity is deep and microstriae are visible.

Discussion. As noted in the discussion of *Utahconus* Miller, the emended diagnosis proposed by Zeballo *et al*. (2005b) and later formalized by Albanesi and Aceñolaza (2005) actually corresponds to the diagnosis of the new genus herein. Because the genus is new, the diagnosis is extended detailing the characteristics of each form. We use the nomenclature proposed by Sweet and Schönlaub (1975) and Sweet (1988) by adding two morphotypes that were previously illustrated by Zeballo *et al*. (2005b, figs. 3.AC, AD).

Tilcarodus humahuacensis (Albanesi and Aceñolaza, 2005)
Figures 7O–U, 10H–Q

1994. *Utahconus* sp. Rao *et al*.: 75; pl. II, fig. 11.
?1994. *Juanognathus* sp. Ji and Barnes: 44, 45; pl. 14, figs 19–22.
2005b. *Utahconus* n. sp A. Zeballo *et al*.: 59, 60; figs. 3. Z–AF.
2005. *Utahconus humahuacensis* Albanesi and Aceñolaza: 306, 307; figs 4.I–O.
2008. *Utahconus humahuacensis* Albanesi and Aceñolaza. Zeballo *et al*.: fig. 3.15.

Material. 194 M elements, 613 Pa elements, 235 Pb elements, 116 Sa elements, 278 Sb elements, 275 Sc elements, 100 Sd elements (CORD-MP 8006/1, 8011/1, 8018/1–7, 8039/1–7, 8061/1–2, 8048/1–78, 8053/1–282, 8062/1–19, 8101/1–140, 8105/1–26, 8118/134, 8120/1–290, 8131/1–40, 11316/1, 16494/1–46, 16498/1–376, 16516/1–6, 16523/1–53, 16529/1–148, 16537/1–13, 16581/1–83, 16614/1–156, 16696/1–4).

Diagnosis. Same as for *Tilcarodus* genus.

Remarks. Zeballo *et al*. (2005b) described the morphotypes of this species assigned to *Utahconus* n. sp. A, which was then formally defined by Albanesi and Aceñolaza (2005). The correspondence between the morphotypes

named by Zeballo *et al*. (2005b), Albanesi and Aceñolaza (2005) and this work is as follows: *a* = Sd, *b* = Sb, *c* = Sa, *e* = M, *f* = Pb. The specimen named in doubt as *c?* (Zeballo *et al*., 2005b, figure. 3.AC) corresponds to the Sc morphotype, and the specimen designated as *f?* (op. cit., figure. 3.AE) belongs to the Pa morphotype.

Discussion. It should be clarified that the material illustrated as *Utahconus* n. sp. A by Zeballo *et al*. (2005b) is an early form of the species, where specimens are smaller and have less ornamentation. The sample from which those specimens were recovered comes from the bottom of the Rupasca Member; i.e. *Cordylodus angulatus* Zone, while illustrations of the same species provided by Albanesi and Aceñolaza (2005) are of a late form, which comes from the middle part of the Rupasca Member, *Paltodus deltifer* Zone (*Paltodus deltifer pristinus* Subzone).

The elements of *Juanognathus* sp. illustrated by Ji and Barnes (1994, plate 14, figures 19–22) are assigned to *Tilcarodus humahuacensis* with doubt, where figure 19 corresponds to the Pa morphotype, figure 20 to the Sb morphotype, and figures 21 and 22 to the M morphotype. Although there are certain morphological differences that could be due to population variations.

Occurrence and age. Alfarcito and Rupasca members, Santa Rosita Formation, Lower Member, Coquena Formation, and Devendeus Formation. *Cordylodus angulatus* Zone–*Paltodus deltifer* Zone (*Paltodus deltifer pristinus* Subzone), early Tremadocian (Tr1)–middle Tremadocian (Tr2), Early Ordovician.

Geographic and stratigraphic distribution. Argentina (Rao *et al*., 1994). *Paltodus deltifer* Zone?, middle Tremadocian (Tr2), Early Ordovician.

Order PRIONIODONTIDA Dzik, 1976
Family ACODONTIDAE Lindström, 1955
Genus *Acodus* Pander, 1856

Type species. *Acodus erectus* Pander, 1856, original designation.

Diagnosis. Although the original material of the type species is missing, the diagnosis of the genus *Acodus* was recently emended by Albanesi *et al*. (2011) with material from the Zenta Range and Incamayo area, south of the Cordillera Oriental of Argentina. The name *Acodus* is maintained and considered as a valid genus due to the uninterrupted use given by diverse authors, with amendments, and to the new collections of the species *Acodus deltatus*, among others, that nominates the eponymous biozone.

Acodus primitivus n. sp.
Figures 6J–P, 10A–G

2008. *Acodus deltatus* Lindström (*sensu lato*). Zeballo *et al*.: fig. 4.7.

Material. 5 M elements, 18 Pa elements, 15 Pb elements, 1 Sa element, 1 Sb element, 1 Sc element, 4 S elements (CORD-MP 16608/1–4, 16631/1, 16635/1–34, 16655/16).

Holotype. Pa acodiform element, CORD-MP 16635/7 (Figure 6K);

Paratype. Pa acodiform element, CORD-MP 16635/19 (Figure 10C).

Derivatio nominis. From Latin *primitivus*: primitive, indicating its appearance before the other species of *Acodus*, e.g. *A. deltatus* Lindström.

Type locality and stratotype. Huacalera, Tilcara Department, Jujuy Province, Argentina. Humacha section, level Hum1, *ca*. 38.50 m above the base of the Humacha Member, Santa Rosita Formation (Figure 4).

Diagnosis. New species of small *Acodus* elements with thin walls, where the Pa element (acodiform) has an external costa on its side; the cusp is suberect to proclined and the height is equal to or less than the length of the oral margin. The Pb element (gothodiform) presents the suberect cusp almost the same size as the oral margin, with two antero-lateral costae that line the anterior side. The remaining morphotypes are less ornate, with weak lateral costae. Microstriae are only discernible with large magnification.

Description. M element: geniculate (oistodiform) morphotype, laterally compressed, keeled anterior and posterior margins, short oral margin and cusp long, with gently curved anterior margin.

Pa element: acodiform morphotype of short cusp, slightly proclined or erect, whose length is similar or less than the length of the oral margin, with a carina or costa which crosses the middle position of the outer lateral side.

Pb element: gothodiform morphotype of proclined cusp, whose length is near the length of the oral margin. Two antero-lateral costae define the anterior side (Figure 10F).

Sa element: symmetrical morphotype, with two lateral costae and a posterior costa, that is lower than the lateral ones, which do not reach the aboral margin.

Sb element: concave–convex element, long base and proclined cusp, whose anterior margin is flexed toward the inner margin.

Sc element: morphotype similar to Sb, except that the anterior margin is not flexed to the inner edge and the base is shorter.

Sd elements were still not recovered, pending descriptions to additional material.

Microstriae are present with different strength and only visible with high magnification (Figure 10E).

Discussion. *Acodus deltatus* Lindström, 1955 differs from the new species described here by having the Pa morphotype with straight anterior margin, the lateral costa restricted to the base, the cusp more proclined, and the oral and aboral margin at almost 90°. Other species of *Acodus*, e.g. *A.*

kechikaensis Pyle and Barnes, 2002, *A. delicatus* Branson and Mehl, 1933, *A. triangularis* (Ding in Wang, 1993), have an increased ornamentation and the M morphotype is clearly geniculate, with a well developed posterior process.

Acodus apex Albanesi and Zeballo, 2011, a recently described species from the Incahuasi section, was recorded in younger strata of the Parcha Formation, south of the Cordillera Oriental (Albanesi *et al*., 2011). This form is probably phylogenetically related, because it has a design similar to *A. primitivus* n. sp., although their cusps are more developed, like the ornamentation of the elements, and the diagnostic Pa morphotype has an erect cusp.

Occurrence and age. Upper part of the Rupasca Member, and Humacha Member, Santa Rosita Formation, and Upper Member, Coquena Formation. *Paltodus deltifer* Zone (*Paltodus deltifer deltifer* Subzone), middle Tremadocian (Tr2), Early Ordovician.

6. DISCUSSION AND CONCLUSIONS

The conodonts recovered from the Santa Rosita Formation in the study area (*ca*. 11 000 elements) indicate the presence of the *Cordylodus intermedius* (*Hirsutodontus simplex* Subzone), *C. lindstromi sensu lato*, *C. angulatus* and *Paltodus deltifer* (*P. d. pristinus* and *P. d. deltifer* subzones) zones. The species described herein occur in the two latter zones.

A total of 5163 conodont specimens provide the basis for the diagnosis of eight new species, and the creation of the new genus *Tilcarodus*, that comprises the type species *T. humahuacensis*. The common features of each morphotype of the species within the genera *Acanthodus* and *Utahconus* (e.g. similarity of the basal contour, size of the bases, inclination of the cusp) and their consecutive appearance along the stratigraphic column, suggest a phylogenetic relationship between them (i.e. *A. raqueli* and *A. humachensis* as well as *U. tortibasis, U. purmamarcensis* and *U. scandodiformis*). The presence of other species of *Variabiloconus* in the study area (e.g. *V. variabilis*, *V. datsonensis*, *V. bicuspatus*) and the similar design of their apparatuses, suggest a possible link between them and the new species *V. crassus*. In the same way, *Acodus primitivus* n. sp. seems to have some connection with *A. apex*, registered in other parts of the Cordillera Oriental.

The whole conodont fauna recorded at the Tilcara Range corresponds to a new province within the Cold Domain of the Shallow-Sea Realm *sensu* Zhen and Percival (2003) (Albanesi *et al*., 2007b; Zeballo *et al*., 2008). Nevertheless, it is also significant for the diversity of forms and the number of elements of the genera *Acanthodus* and *Utahconus* in the sandy sequences. This assemblage is common in the Tropical Domain and it refers to shallow waters palaeoenvironments (Ji and Barnes, 1994; Ortega and Albanesi, 2005). A detailed approach to the synecological and palaeobiogeographical aspects of the conodont fauna is carried out by Zeballo and Albanesi (2013).

ACKNOWLEDGEMENTS

The authors wish to thank the ANPCyT, Argentina, for its support through FONCyT, PICT 07-15076 and 2008-1797. G. L. Albanesi gratefully acknowledges CONICET for the continuing support to the study of conodonts, and to the Universidad Nacional de Córdoba, where this study was accomplished. He specially thanks the Guggenheim Foundation. Dr Yong-Yi Zhen and an anonymous reviewer amended this contribution. We thank them and Ian Somerville for their valuable suggestions. The conodont microphotographs were taken at the Laboratorio de Microscopía (LAMARX) of the Universidad Nacional de Córdoba. This work is a contribution to IGCP Project 591.

REFERENCES

Aceñolaza, F.G. 1983. The Tremadocian beds and the Cambrian–Ordovician boundary problems in Latin America. *Papers for the Symposium on the Cambrian–Ordovician and Ordovician–Silurian Boundaries*, Nanjing Institute of Geology and Palaeontology, Academia Sinica, 88–93.

Aceñolaza, F.G., Aceñolaza, G.F. 1992. The genus *Jujuyaspis* as a world reference fossil for the Cambrian–Ordovician boundary. In: *Global Perspectives on Ordovician Geology*, Webby, B.D., Laurie, J.R. (eds). Balkema, Rotterdam, 115–120.

Agematsu, S., Sashida, K., Salyapongse, S., Sardsud, A. 2008. Early Ordovician conodonts from Tarutao island, southern peninsular Thailand. *Palaeontology* **51**, 1435–1453.

Albanesi, G.L., Aceñolaza, F.G. 2005. Conodontes de la Formación Rupasca (Ordovícico Inferior) en el Angosto de Chucalezna, Cordillera Oriental de Jujuy: nuevos elementos bioestratigráficos para una localidad clásica del noroeste argentino. *Ameghiniana* **42**, 295–310.

Albanesi, G.L., Zeballo, F.J., Monaldi, C.R., Ortega, G. 2007a. La Zona de conodontes de *Paroistodus proteus—Acodus deltatus* y graptolitos asociados en el Tremadociano superior del noroeste argentino. *Ameghiniana (Resúmenes)* **44**, 87–88R.

Albanesi, G.L., Zeballo, F.J., Bergström, S.M. 2007b. The *Paltodus deltifer* Zone (late Tremadocian; Early Ordovician) in Argentina: new conodont data for intercontinental correlation and paleobiogeographic analysis. In: *Acta Paleontologica Sinica (suppl.)* Li, J., Fan, J., Percival, I.G. (eds). **46**, 16–22.

Albanesi, G.L., Ortega, G., Zeballo, F.J. 2008. Faunas de conodontes y graptolitos del Paleozoico Inferior en la Cordillera Oriental argentina. In: *Geología y Recursos Naturales de la provincia de Jujuy. Relatorio del 17° Congreso Geológico Argentino*, Coira, B., Zapettini, E.O. (eds). Jujuy, 98–118.

Albanesi, G.L., Ortega, G., Monaldi, C.R., Zeballo F.J. 2011. Conodontes y graptolitos del Tremadociano tardío de la sierra de Zenta, Cordillera Oriental de Jujuy, Argentina. *Ameghiniana* **48**, 242–263.

Amengual, R., Zanettini, J.C. 1974. Geología de la quebrada de Humahuaca entre Uquía y Purmamarca (provincia de Jujuy). *Revista de la Asociación Geológica Argentina* **39**, 30–40.

An, T.-X., Zhang, F., Xiang, W., Zhang, Y., Xu, W., Zhang, H., Jiang, D., Yang, C., Lin, Y.-K., Cui, Z., Yang, X. 1983. *The Conodonts of North China and the Adjacent Regions*. Science Press: Beijing, 1–223.

Astini, R.A. 2003. The Ordovician Proto-Andean Basins. In: *Ordovician Fossils of Argentina*, Benedetto, J.L. (ed.). Secretaría de Ciencia y Tecnología, Universidad Nacional de Córdoba: Córdoba, 1–74.

Astini, R.A. 2008. Sedimentación, facies, discordancias y evolución paleoambiental durante el Cambro-Ordovícico. In: *17° Congreso Geológico Argentino*, Coira, B., Zapettini, E. (eds). Jujuy, Relatorio, 50–73.

Bateson, W. 1885. The ancestry of the Chordata. *Quarterly Journal of Microscopical Science* **26**, 218–571.

Bergström, S.M., **Chen, X.**, **Gutiérrez Marco, J.C.**, **Dronov, A. 2009**. The new chronostratigraphic classification of the Ordovician System and its relations to major regional series and stages and to $\delta^{13}C$ chemostratigraphy. *Lethaia* **42**, 97–107.

Bonarelli, G. 1921. Tercera contribución al conocimiento geológico de las regiones petrolíferas subandinas del norte, Provincias de Salta y Jujuy. *Anales del Ministerio y Agricultura, Sección Geología, Mineralogía y Minería* **15**, 1–98.

Brackebusch, L. 1883. Estudio sobre la Formación Petrolífera de Jujuy. *Boletín de la Academia Nacional de Ciencias (Córdoba)* **5**, 137–252.

Brackebusch, L. 1892. Die Kordillerenpaesse zwischen der Argentinischen Republik und Chile, von 22°–35° S. *Br. Zeitschrift Deutsche Gesellschaft für Erdkunde* **27**, 250–348.

Branson, E.B. 1938. Stratigraphy and paleontology of the Lower Mississippian of Missouri, part 1. *University of Missouri Studies* **29**, 1–208.

Branson, E.B., **Mehl, M.G. 1933**. Conodont studies, numbers 1 and 2. *University of Missouri Studies* **8**, 1–349.

Buatois, L.A., **Zeballo, F.J.**, **Albanesi, G.L.**, **Ortega, G.**, **Vaccari, N.E.**, **Mángano, M.G. 2006**. Depositional environments and stratigraphy of the Upper Cambrian–Lower Ordovician Santa Rosita Formation at the Alfarcito area, Cordillera oriental, Argentina: integration of biostratigraphic data within a sequence stratigraphic framework. *Latin American Journal of Sedimentology and Basin Analysis* **13**, 1–29.

Chen, J.-Y., Gong, W.-L. 1986. Conodonts. In: *Aspects of Cambrian–Ordovician Boundary Interval in Dayangcha, China*, Chen, J.-Y. (ed.). China Prospect Publishing House: Beijing, 93–223.

Druce, E.C., **Jones, P.J. 1971**. Cambro-Ordovician conodonts from the Burke River Structural Belt, Queensland. *Bureau of Mineral Resources, Geology and Geophysics Bulletin* **110**, 1–159.

Dzik, J. 1976. Remarks on the evolution of Ordovician conodonts. *Acta Palaeontologica Polonica* **21**, 395–455.

Fahraeus, L.E., **Roy, K. 1993**. Conodonts from the Cambro-Ordovician Cooks Brook and Middle Arm Point Formations, Bay of Islands, western Newfoundland. *Geologica et Palaeontologica* **27**, 1–53.

Feruglio, E. 1931. Observaciones geológicas en las provincias de Salta y Jujuy. *Contribución a la Primera Reunión Nacional de Geografía* **7**, 1–39.

Furnish, W.M. 1938. Conodonts from the Prairie du Chien beds of the upper Mississippi Valley. *Journal of Paleontology* **12**, 318–340.

Groeber, P. 1938. *Mineralogía y Geología*. Espasa-Calpe Argentina: Buenos Aires, 1–492.

Harrington, H.J., **Leanza, A.F. 1957**. *Ordovician Trilobites of Argentina*. Department of Geology, University of Kansas Press: Lawrence, 1–276.

Hausen, J. 1925. Sobre un perfil geológico en el borde oriental de la Puna de Atacama, con una descripción de algunos yacimientos minerales en la Puna de Salta y Jujuy. *Boletín de la Academia Nacional de Ciencias (Córdoba)* **28**, 1–95.

Jeppsson, L., **Anheus, R.**, **Fredholm, D. 1999**. The optimal acetate buffered acetic acid technique for extracting phosphatic fossils. *Journal of Paleontology* **73**, 964–972.

Ji, Z., **Barnes, C.R. 1994**. Lower Ordovician conodonts of the St. George Group, Port au Port Peninsula, western Newfounland, Canada. *Palaeontographica Canadiana* **11**, 1–149.

Jones, P.J. 1971. Lower Ordovician conodonts from the Bonaparte Gulf Basin and the Daly River Basin, northwestern Australia. *Bureau of Mineral Resources, Geology and Geophysics Bulletin* **117**, 1–98.

Keidel, J. 1910. Estudios geológicos en la quebrada de Humahuaca y en la de Iruya y en algunos de sus valles laterales (Provincias de Jujuy y Salta). *Anales del Ministerio de Agricultura, Sección Geología, Mineralogía y Minería* **5**, 76–77.

Keidel, J. 1943. El Ordovícico de los Andes del Norte Argentino y sus depósitos marino-glaciales. *Boletín de la Academia Nacional de Ciencias (Córdoba)* **36**, 140–229.

Landing, E., **Barnes, C.R.**, **Stevens, R.K. 1986**. Tempo of earliest Ordovician graptolite faunal succession: conodont-based correlations from the Tremadocian of Quebec. *Canadian Journal of Earth Sciences* **23**, 1928–1949.

Landing, E., **Westrop, S.R.**, **Knox, L.A. 1996**. Conodonts, stratigraphy, and relative sea-level changes of the Tribes Hill Formation (Lower Ordovician, East-Central New York). *Journal of Paleontology* **70**, 656–680.

Landing, E., **Westrop, S.R.**, **Van Aller Hernick, L. 2003**. Uppermost Cambrian–Lower Ordovician faunas and Laurentian platform sequence stratigraphy, Eastern New York and Vermont. *Journal of Paleontology* **71**, 78–98.

Lindström, M. 1955. Conodonts from the lowermost Ordovician strata of south-central Sweden. *Geologiska Föreningens i Stockholm Förhandlingar* **76**, 517–604.

Lindström, M. 1970. A suprageneric taxonomy of the conodonts. *Lethaia* **3**, 427–445.

Löfgren, A.M., **Repetski, J.E.**, **Ethington, R.L. 1999**. Some trans-Iapetus conodont faunal connections in the Tremadocian. *Bollettino della Società Paleontologica Italiana* **37**, 159–173.

López, C.R., **Nullo, F.E. 1969**. Geología de la margen izquierda de la quebrada de Humahuaca, de Huacalera a Maimará, Departamento Tilcara, Provincia de Jujuy, Argentina. *Revista de la Asociación Geológica Argentina* **24**, 173–182.

Miller, J.F. 1969. Conodont fauna of the Notch Peak Limestone (Cambro-Ordovician), House Range, Utah. *Journal of Paleontology* **43**, 413–439.

Miller, J.F. 1980. Taxonomic revisions of some Upper Cambrian and Lower Ordovician conodonts with comments on their evolution. *University of Kansas Paleontological Contributions* **99**, 1–44.

Moya, M.C. 1988a. *Estratigrafía del Tremadociano en el tramo austral de la Cordillera Oriental argentina*. Ph.D Thesis, Universidad Nacional de Salta.

Moya, M.C. 1988b. Lower Ordovician in the southern part of the argentine Eastern Cordillera. *Lecture Notes in Earth Sciences* **17**, 55–69.

Moya, M.C. 2008. El Paleozoico Inferior en el noroeste argentino. Evidencias, incógnitas, propuestas para la discusión. In: *Geología y Recursos Naturales de la provincia de Jujuy. Relatorio del 17° Congreso Geológico Argentino, Jujuy*, Coira, B., Zapettini, E.O. (eds). 74–84.

Moya, M.C., **Malanca, S.**, **Monteros, J.A.**, **Albanesi, G.L.**, **Ortega, G.**, **Buatois, L.A. 2003**. The Angosto del Moreno Area, Eastern Cordillera, Jujuy Province. In: *Ordovician and Silurian of the Cordillera Oriental and Sierras Subandinas, NW Argentina*, Aceñolaza, G.F. (ed.). INSUGEO, Miscelánea **11**, 29–35.

Nicoll, R.S. 1991. Differentiation of Late Cambrian–Early Ordovician species of *Cordylodus* (Conodonta) with biapical basal cavities. *Bureau of Mineral Resources, Journal of Australian Geology and Geophysics* **12**, 223–244.

Nicoll, R.S., **Miller, J.F.**, **Nowlan, G.S.**, **Repetski, J.E.**, **Ethington, R.L. 1999**. *Iapetonudus* (N. gen.) and *Iapetognathus* Landing, unusual earliest Ordovician multielement conodont taxa and their utility for biostratigraphy. *Brigham Young University Geology Studies* **44**, 27–101.

Ortega, G., **Albanesi, G.L. 2005**. Tremadocian graptolite-conodont biostratigraphy of the South American Gondwana margin (Eastern Cordillera, NW Argentina). *Geologica Acta* **3**, 355–371.

Pander, C.H. 1856. *Monographie der Fossilen Fische des Silurischen Systems der Russisch-Baltischen Gouvernements*. Akademie der Wissenschaften: San Petersburgo, 1–91.

Pokorny, V. 1963. In: *Principles of Zoological Micropalaeontology*, Ingerson, E. (ed.). International Series of Monographs on Earth Sciences, Pergamon Press: Oxford; 652.

Pyle, J.L., **Barnes, C.R. 2002**. *Taxonomy, Evolution, and Biostratigraphy of Conodonts from the Kechika Formation, Skoki Formation, and Road River Group (Upper Cambrian to Lower Silurian), Northeastern British Columbia*. NRC Research Press: Ottawa, 1–227.

Ramos, V.A. 1999. Las provincias geológicas del territorio argentino. In: *Geología Argentina*, Caminos, R. (ed.). Instituto de Geología y Recursos Minerales, SEGEMAR: Buenos Aires, 41–96.

Rao, R.I. 1999. Los conodontes cambro-ordovícicos de la sierra de Cajas y del Espinazo del Diablo, Cordillera Oriental, República Argentina. *Revista Española de Micropaleontología* **31**, 5–20.

Rao, R.I., **Flores, F.J. 1998**. Conodontes ordovícicos (Tremadoc superior) de la sierra de Aguilar, provincia de Jujuy, *República Argentina. Bioestratigrafía y Tafonomía. Revista Española de Micropaleontología* **30**, 5–20.

Rao, R.I., **Hünicken, M.A. 1995**. Conodontes del Cámbrico Superior–Ordovícico Inferior en el área de Purmamarca, Cordillera Oriental, Provincia de Jujuy, R. Argentina. *Boletín de la Academia Nacional de Ciencias (Córdoba)* **60**, 249–266.

Rao, R.I., **Tortello, M.F. 1998**. Tremadoc conodonts and trilobites from the Cardonal Formation, Incamayo Creek, Salta Province, northwestern Argentina. In: *Proceedings of the 6th European Conodont Symposium (ECOS VI)*, Szaniawski, H. (ed.). *Palaeontologia Polonica* **58**, 31–45.

Rao, R., **Hünicken, M.**, **Ortega, G. 1994**. Conodontes y graptolitos del Ordovícico Inferior (Tremadociano–Arenigiano) en el área de Purmamarca, provincia de Jujuy, Argentina. *Anais Academia Brasileria de Ciencias* **66**, 59–83.

Schlagintweit, O. 1937. Observaciones estratigráficas en el norte argentino. *Boletín de Información Petrolífera* **14**, 1–49.

Serpagli, E., **Ferretti, A.**, **Nicoll, R.S.**, **Serventi, P. 2008**. The conodont genus *Teridontus* (Miller, 1980) from the early Ordovician of Montagne Noire, France. *Journal of Paleontology* **82**, 612–620.

Stone, J. 1987. Review of investigative techniques used in the study of conodonts. In: *Conodonts: Investigative Techniques and Applications*, Austin, R.L. (ed.). Ellis Horwood Limited: Chichester, 7–34.

Sweet, W.C. 1988. The Conodonta. *Oxford Monographs on Geology and Geophysics* **10**, 1–212.

Sweet, W.C., **Schönlaub, H.P. 1975**. Conodonts of the genus *Oulodus* Branson and Mehl, 1933. *Geologica et Palaeontologica* **9**, 41–59.

Tolmacheva, T.J., **Abaimova, G.P. 2009**. Late Cambrian and Early Ordovician conodonts from the Kulumbe River section, northwest Siberian Platform. *Memoirs of the Association of Australasian Palaeontologists* **37**, 427–451.

Tortello, M.F., **Rao, R.I. 2000**. Trilobites y conodontes del Ordovícico temprano del Angosto de Lampazar (Provincia de Salta, Argentina). *Boletín Geológico y Minero* **111**, 61–84.

Tortello, M.F., **Rábano, I.**, **Rao, R.**, **Aceñolaza, F.G. 1999**. Los trilobites de la transición Cámbrico–Ordovícico en la quebrada Amarilla (Sierra de Cajas, Jujuy, Argentina). *Boletín Geológico y Minero* **110**, 555–572.

Turner, J.C.M., **Mon, R. 1979**. Cordillera Oriental. In: *Segundo Simposio de Geología Regional Argentina*, Turner, J.C.M. (ed.). Academia Nacional de Ciencias, Córdoba, **Tomo 1**, 57–94.

Vaccari, N.E., **Waisfeld, B.G.**, **Marengo, L.**, **Smith, L. 2010**. *Kainella* Walcott, 1925 (Trilobita, Ordovícico Temprano) en el noroeste de Argentina y sur de Bolivia. Importancia bioestratigráfica. *Ameghiniana* **47**, 293–305.

Viira, V. 1970. Konodonty Varanguskoj pachki (Verchnij Tremadok Estonii) [Conodonts of the Varangu Member (Estonian upper Tremadoc)]. *Eesti NSV Teaduste Akadeemia, Keemia-Geoloogia* **19**, 224–233.

Waisfeld, B.G., **Vaccari, N.E. 2008**. Bioestratigrafía de trilobites del Paleozoico Inferior de la Cordillera Oriental. In: *Geología y Recursos Naturales de la provincia de Jujuy*. *Relatorio del 17° Congreso Geológico Argentino*, Coira, B., Zapettini, E.O. (eds). Jujuy, 119–127.

Wang, C.Y. (ed.). 1993. *Conodonts of the Lower Yangtze Valley—an Index to Biostratigraphy and Organic Metamorphic Maturity*. Science Press: Beijing; 1–326. (in Chinese with English summary).

Zeballo, F.J., **Albanesi, G.L. 2009**. Conodontes cámbricos y *Jujuyaspis keideli* Kobayashi (Trilobita) en el Miembro Alfarcito de la Formación Santa Rosita, quebrada de Humahuaca, Cordillera Oriental de Jujuy. *Ameghiniana* **46**, 537–556.

Zeballo, F.J., **Albanesi, G.L. 2013**. Biofacies and palaeoenvironments of conodonts from the Cambro-Ordovician sequences of the quebrada de Humahuaca, Cordillera Oriental of Jujuy, Argentina. *Geological Journal* **48**(2–3), 194–211. DOI: 10.1002/gj2435

Zeballo, F.J., **Tortello, M.F. 2005**. Trilobites del Cámbrico tardío–Ordovícico temprano del área de Alfarcito, Tilcara, Cordillera Oriental de Jujuy, Argentina. *Ameghiniana* **42**, 125–140.

Zeballo, F.J., **Albanesi, G.L.**, **Ortega, G. 2005a**. Conodontes y graptolitos de las formaciones Alfarcito y Rupasca (Tremadociano) en el área de Alfarcito, Tilcara, Cordillera Oriental de Jujuy, Argentina. Parte 1: Bioestratigrafía. *Ameghiniana* **42**, 39–46.

Zeballo, F.J., **Albanesi, G.L.**, **Ortega, G. 2005b**. Conodontes y graptolitos de las formaciones Alfarcito y Rupasca (Tremadociano) en el área de Alfarcito, Tilcara, Cordillera Oriental de Jujuy, Argentina. Parte 2: Paleontología sistemática. *Ameghiniana* **42**, 47–66.

Zeballo, F.J., **Albanesi, G.L.**, **Ortega, G. 2008**. New late Tremadocian (Early Ordovician) conodont and graptolite records from the southern South American Gondwana margin (Eastern Cordillera, Argentina). *Geologica Acta* **6**, 131–145.

Zeballo, F.J., **Albanesi, G.L.**, **Ortega, G. 2011**. Biostratigraphy and paleoenvironments of the Santa Rosita Formation (Late Furongian–Tremadocian), Cordillera Oriental of Jujuy, Argentina. In: *Ordovician of the World*, Gutiérrez-Marco, J.C., Rábano, I., García-Bellido, D. (eds). Instituto Geológico y Minero de España, Madrid, Cuadernos del Museo Geominero **14**, 625–632.

Zhen, Y.-y., **Percival, I.G. 2003**. Ordovician conodont biogeography—reconsidered. *Lethaia* **36**, 357–370.

APPENDIX

Table 1. Absolute frequency of the new conodont species described in this paper (samples from the northern area).

SPECIES / SAMPLES / Mass [gr]	ElAr1 2440	ElArA 2275	ElArB 2870	ElArC 1565	ElArD 2830	ElArE 1795	ElArF 3355	TrCi1a 3015	TrCi1b 2645	Hum0 1100	Hum1 3150	Hum2 3960	Hum3 2215	Hum6 2430	Moya2 2105	Chuc6 1740	Chuc8 1790	Chuc11 2815	TOTAL
Acanthodus humachensis n. sp.											265	22	4						291
Acanthodus raqueli n. sp.		505		14										1					520
Acodus primitivus n. sp.										1	34	6							41
Kallidontus gondwanicus n. sp.		4	16																20
Tilcarodus humahuacensis		46	376	5	53	148	13												641
Utahconus scandodiformis n. sp.										2	347	56	4						409
Utahconus tortibasis n. sp.		568		24															592
Variabiloconus crassus n. sp.	17	238	50	12				7	7						44	11	45	28	459
TOTAL	17	1361	442	55	53	148	13	7	7	3	646	84	8	1	44	11	45	28	**2973**

Table 2. Absolute frequency of the new conodont species described in this paper (samples from the southern area).

SPECIES / SAMPLES / Mass[gr]	CC1 1930	CC2 2210	CC3 2490	CC4 2430	CC5 2380	CC8 1660	CC9 2000	CC11 2150	SG4 3370	SG7A 1250	SG7B 2020	SG7C 1980	SG8 1860	SG9 1550	SG10 2050	PtaCorral1 2200	PtaCorral2 2580	Coq1 1040	CoqSup 2320	Coq2 4170	Coq3 2950	Chal1 4190	Tramp2 825	Tramp3 825	TOTAL
Acanthodus humachensis n. sp.																					28				28
Acanthodus raqueli n. sp.	2			49													32		49	5		47	18		202
Acodus primitivus n. sp.																					4				4
Kallidontus gondwanicus n. sp.						1	2				2			3	3				2	7		1			21
Tilcarodus humahuacensis	1	1	7	7	2	78	282	19			140	26	34	290	40				83			156	4		1170
Utahconus purmamarcensis n. sp.																			73	13		33			119
Utahconus scandodiformis n. sp.																					40				40
Utahconus tortibasis n. sp.	10		18	89						2	57	22											41		239
Variabiloconus crassus n. sp.	13		14	48	7	117	40		6	1	35	2				5		5					23	51	367
TOTAL	26	1	39	193	9	196	324	19	6	3	234	50	34	293	43	5	32	5	207	25	72	237	86	51	**2190**